Thesis for the Degree of Master of Science

Petrological study on the low-grade metamorphic rocks from Gogunsan Islands

by

Min Ju Yang

Department of Environmental Geosciences

The Graduate School

Pukyong National University

February, 2009

Petrological study on the low-grade metamorphic rocks from Gogunsan Islands

고군산군도 지역에 분포하는 저변성도 변성암류의 암석학적 연구

Advisor: Yong Sun Song

by

Min Ju Yang

A thesis submitted in partial fulfillment of the requirements
for the degree of Master of science

in the Department of Environmental Geosciences,
The Graduate School,
Pukyong National University

February, 2009

Petrological study on the low-grade metamorphic rocks from Gogunsan Islands

A Thesis

by

Min Ju Yang

Approved by:

(Chairman) Key Hun Park

(Member) Yong Sun Song

(Member) Young Seog Kim

February, 2009

양민주의 이학박사 학위논문을 인준함

2009년 2월 25일

주 심 이학박사 박 계 헌 인

위 원 이학박사 송 용 선 인

위 원 이학박사 김 영 석 인

Contents

List of Figures

List of Tables

고군산군도지역에 분포하는 저변성도 변성암류의 암석학적 연구

양 민 주

부경대학교 대학원 환경지질과학과

요 약

전라북도 군산시 고군산군도 북부지역 섬들에 분포하고 있는 저변성도 변성암들에 대한 암석학적 및 지구화학적 연구를 수행하였으며, 변성광물에 대한 EPMA 분석을 병행하였다. 서에서 동으로 가면서 말도, 명도, 방축도 그리고 횡경도에 이르는 고군산군도 북부지역의 섬들은 사질 변성퇴적암층으로 구성되어 있고, 변성염기성암층과 소량의 변성화강암이 수반된다.

연구지역의 변성퇴적암층은 후기의 변형 및 변성작용으로 습곡과 스러스트 듀플렉스 등의 변형구조가 두드러지게 발달되었지만 층리와 사층리, 점이층리 등의 일차적인 퇴적구조를 잘 보존하고 있다.

변성퇴적암과 변성화강암, 변성염기성암의 지구화학적 특성은 연구지역의 변성퇴적층은 대륙주변부에서 비롯된 규산질 쇄설성 퇴적물 기원이며, 화산호 환경에서 칼크알칼리계열 화산활동과 화강암질 심성활동이 수반되었음을 지시한다.

변성퇴적암의 변성광물조합은 녹니석 + 백운모 + 석영 +사장석 (조장석)이고, 변성화강암은 석영 + K-장석 + 사장석(조장석) + 백운모이며, 변성염기성암은 각섬석 (양기석-쳐마카이트) + 사장석(조장석)이다. 이들 암석의 광물조합은 녹색편암상의 변성작용을 지시한다.

변성염기성암에 대해 지질온도압력계에 의해 계산된 온도-압력 조건은 대략 2~4 kbar, 350℃ 정도이다.

이상의 연구지역에 분포된 변성암층에 대한 암석기재적 특성과 변성작용 특성에 의하면 연구지역인 고군산군도 일대에 분포된 변성암층들은 신원생대 지층에 대비될 것으로 추정된다.

1. Introduction

Gogunsan Islands (Archipelago) located about 50km away from Gunsan city to the west (Fig. 1) consist of a few tens of islands including Sinsido, Munyeodo, Seonyudo, Jangjado, Daejangdo and Gwanrido in the south and Maldo, Myeongdo, Bangchukdo, and Hoeonggyeongdo in the north. They are famous for scenic beauty and fantastic rocks.

In the northern part of this islands, spectacular folded beddings of metasedimentary formations are exposed along the coast lines of the islands of Maldo, Myeongdo, Bangchukdo and Hoeonggyeongdo linearly lying west to east. The metamorphic formations are considered as Precambrian in age despite the absence of any considerable evidence (KIGAM, 1995; CHA, 2007).

According to the previous study (e.g. KIGAM, 2004), Precambrian bedrocks are suffered from excessive deformation, more than five times metamorphism, and three times volcanism. But there is no detail studies. Precambrian metamorphic rocks in the Korea Peninsula are suffered from high-graded metamorphism. However, Precambrian rocks in this area suffered from low-graded metamorphism.

This study focused on field occurrence, petrology and geochemistry of the metamorphic rocks from these islands, especially Maldo and Myeongdo, together with EPMA analyses of metamorphic minerals to evaluate P-T conditions of metamorphism and to constrain the tectonic environment of sedimentation and igneous activity and the age of the

rock formations.

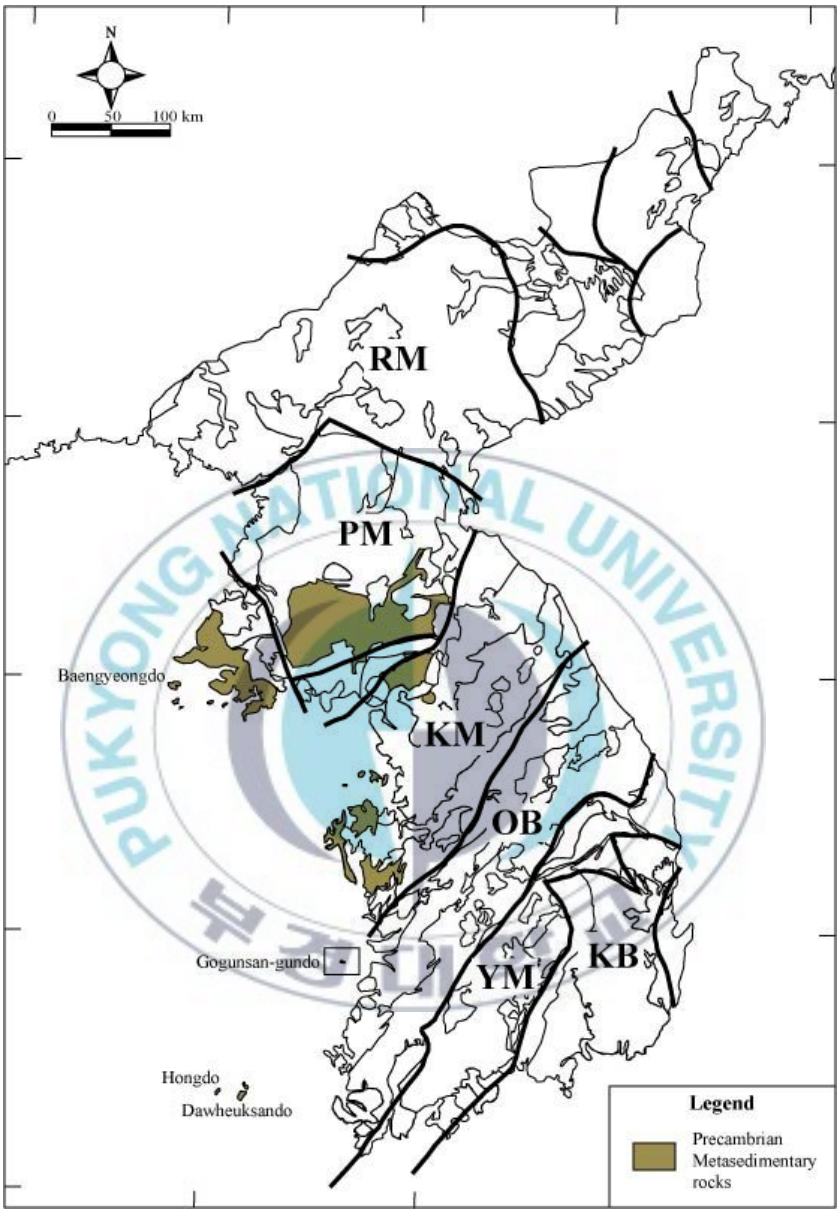

Fig. 1. Tectonic map of Korea showing the distribution of Neoproterozoic metasedimentary formations. (RM, Rangrim Massif; PM, Pyongan Massif; KM, Kyonggi Massif; YM, Yongnam Massif; OB, Okcheon folded Belt; KB, Kyongsang Basin)

2. General geology

In the 1/one million geological map (KIGAM, 1995), Mesozoic formation is indicated to form from Triassic to Cretaceous in Gogunsan islands moreover, Maldo and Myeongdo are distributed Jurassic and Triassic (J1) but the detailed geology is not known.

In the 1/250 thousand geological map (KIGAM; 1973), Gogunsan islands is formed as granite gneiss (grgn) its detailed geology is also not known.

If integrated between two geological maps which are mentioned, it can be summary that Mesozoic sedimentary rocks are formed based on the metamorphic rocks of Precambrian.

Most of Daeheuksando and Hongdo located Yellow Sea are formed as the metamorphic rocks of Precambrian and mid ~ late Proterozoic is revealed in Jeonnam Haenam~Ganggin, Jeonbuk Sunchang~Jinan, Jeonnam Yeonggwang and Jangseong portions and Chungnam Taean (KIGAM, 1995). In these study areas, the study of the Galdu formation of the metasedimentary rocks (Precambrian) was conducted. This Galdu formation is clastic sedimentary rocks and shows to be lower than the LT/HP Regional metamorphism of geologic era (Kim et al., 2000, 2001).

Lim et al. (1999) was studied about the sedimentology of proterozoic's portion in Bangyeongdo and Chungnam Taean. Bangyeon Groups in Bangyeongdo are compared with Sangwon system and Taean Formations in Taean area are almost formed as clastic sedimentary rocks. The metasedimentary in Daeheuksando studied by Lim et al

(1999) is contributed in Sim-li of southeastern area and is laregly composed of Metapelite and Metapsammite. Bangyeong Groups, Taean and Sim-li Formation are represented lower metamorphism than mid ~ late proterozoic. Also, Bangyeongdo Groups and Sim-li Formation alternate the same formation by folds, small faults as well as primary structure particularly (Kim. 1993, Lim. 1999).

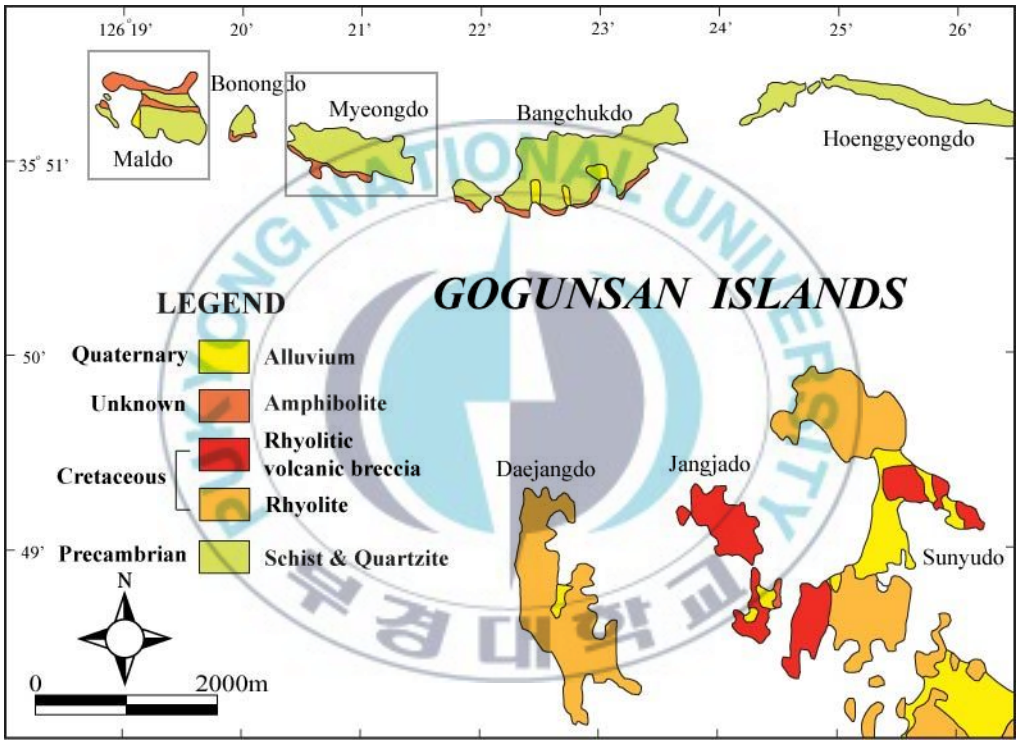

Fig. 2. Geological map of Gogunsan islands modified after Kim et al. (2003).

3. Petrography

Geology of the northern part of the Gogunsan Islands mostly consists of psammitic metasedimentary rocks associated with intercalated metabasite layers and small amount of meta-granites.

3-1. Maldo

The geology of Maldo consists of quartzite, meta-sandstone and dark-gray phyllite intercalated by the formal two rocks (metasedimentary rocks) in Precambrian which is contrasted with Ockchen metamorphic belt and meta-granites in Mesozoic(?) and metabasites of unknown age (Fig. 3).

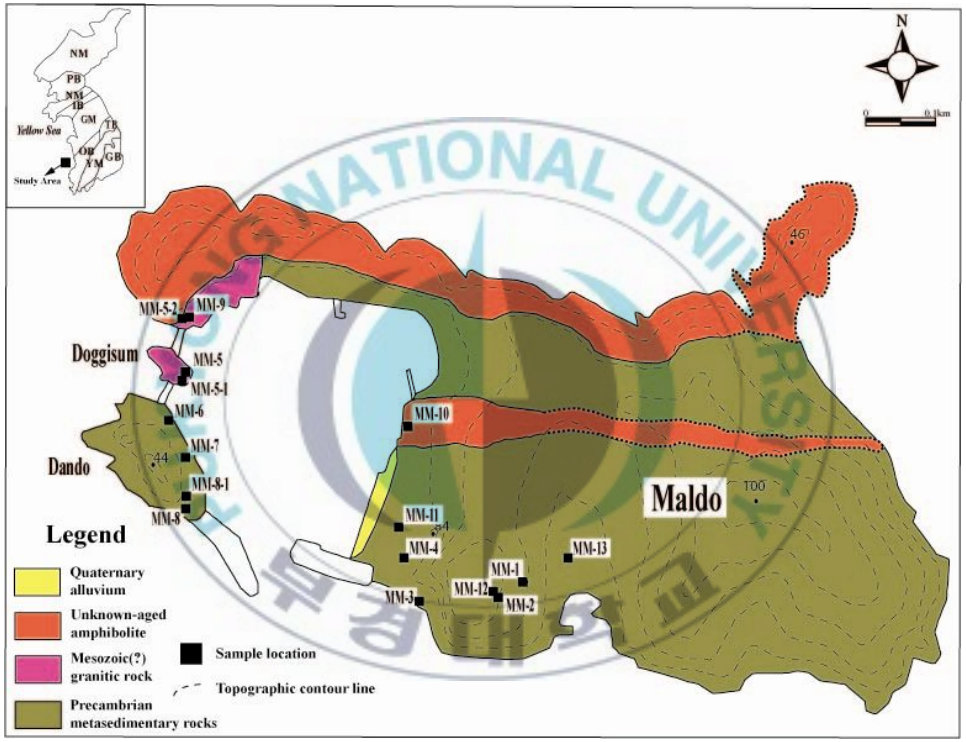

Fig. 3. Geological sketch map of the Maldo.

3-1-1. Metasedimentary rocks

Metasedimentary rocks are distributed in the main island and classify sandstone quartzited and schist or phyllited pelite. the sandstone whose sorting is poorly sorted is consisted of circular coarse sand (2-4mm) and is observed primary structures (bedding, small graded bedding and cross-bedding). The cross-bedding consists of curved cross-bedding sets (thickness : several cm), flows to one way. Also, the one set erodes under 2 or 3 sets (Fig. 4c.), cross-bedding which has a high gradient is showing pushed appearance just after depositing. A primary structure developed well conserves the original shape so we can suppose that it was suffered from just digenesis and consists of only sandy sedimentary. Moreover, due to developing cross-bedding, it is a shallow see origin. Pelite become schist or phyllite and figures out in quartzited sandstone. The strike and dip of schistosity is N58-68°W, 65~84°NE, respectively. This sandstone and pelite constitute alternated bed (or alternation of strata) and show microstructures related to diverse fold and fault structures. This folds are the one sort of secondary folding structure mainly having 70°-280° of fold axis and are suffered over three times folding. By this folding, diverse geologic structures are revealed in limited outcrop scale and the shape of parallel and similar fold depending on a property of matter.

Quartz and muscovite are the main materials adding to little plagioclase (albite), chlorite, iron bearing minerals under the microscope. Under the thin section, all minerals has regular foliation. Quartz's

surface is clean and the straight extinction quartz in the monocrystalline quartz is a little more superior to undulatory extinction quartz as well as its particle is revealed to be extended. Also, microgranular quartz aggregates recrystallizated are being scattered between the edge of quartz and muscovite particle. Muscovites exists matrix's shape with feldspar. Some of them are recrystallized muscovites which are curved, it is because of digenesis. A little felspar which it is almost plagioclase is altered due to albitization. Sometimes its outline is not clear under the microscope and there are plentifully microgranular muscovites and clay mineral. Amphiboles are chloritization (Fig. 6). Iron bearing minerals includes pyrite, chalcopyrite which is acid iron bearing minerals ilmenite.

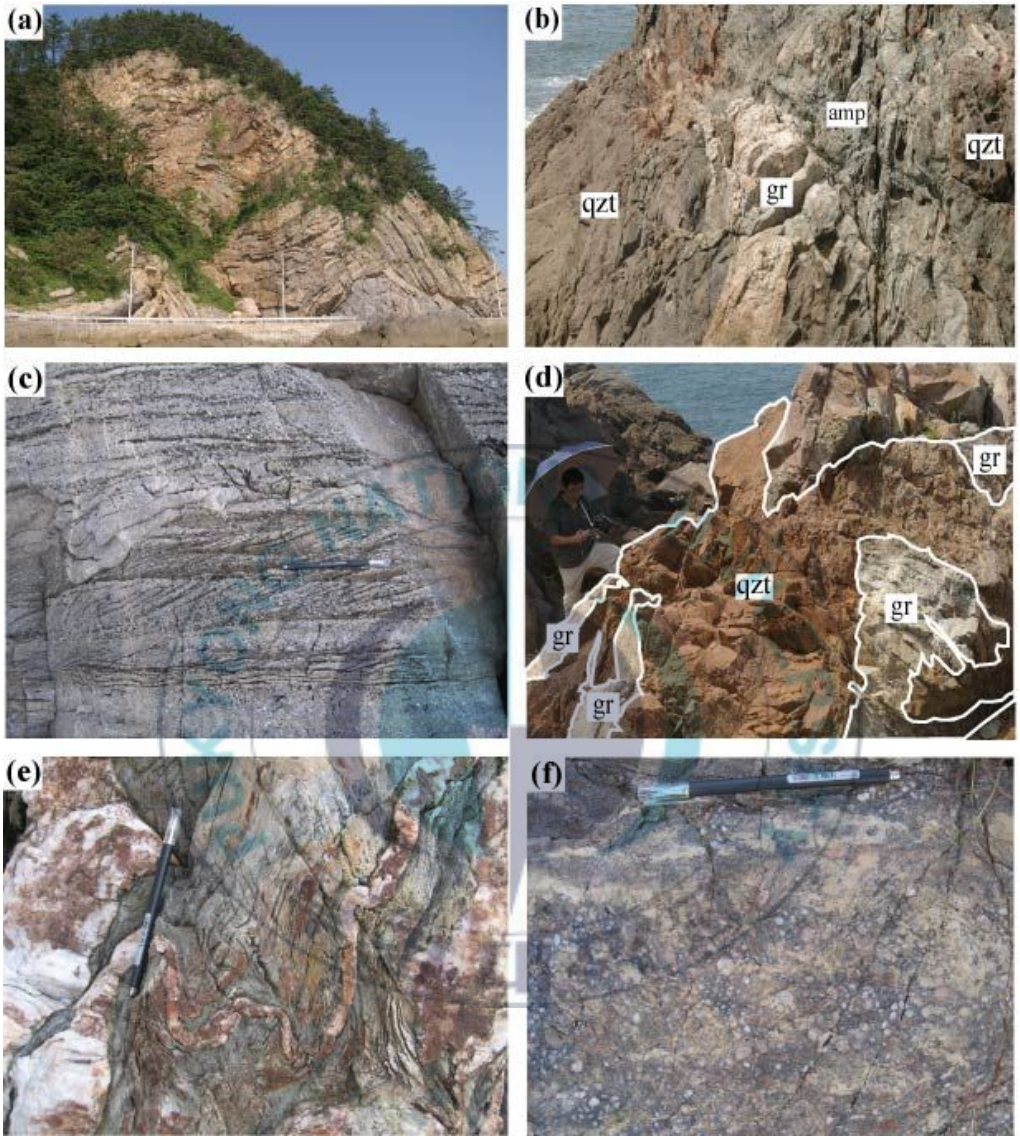

Fig. 4. Outcrop photographs of the metamorphic rocks of Maldo.

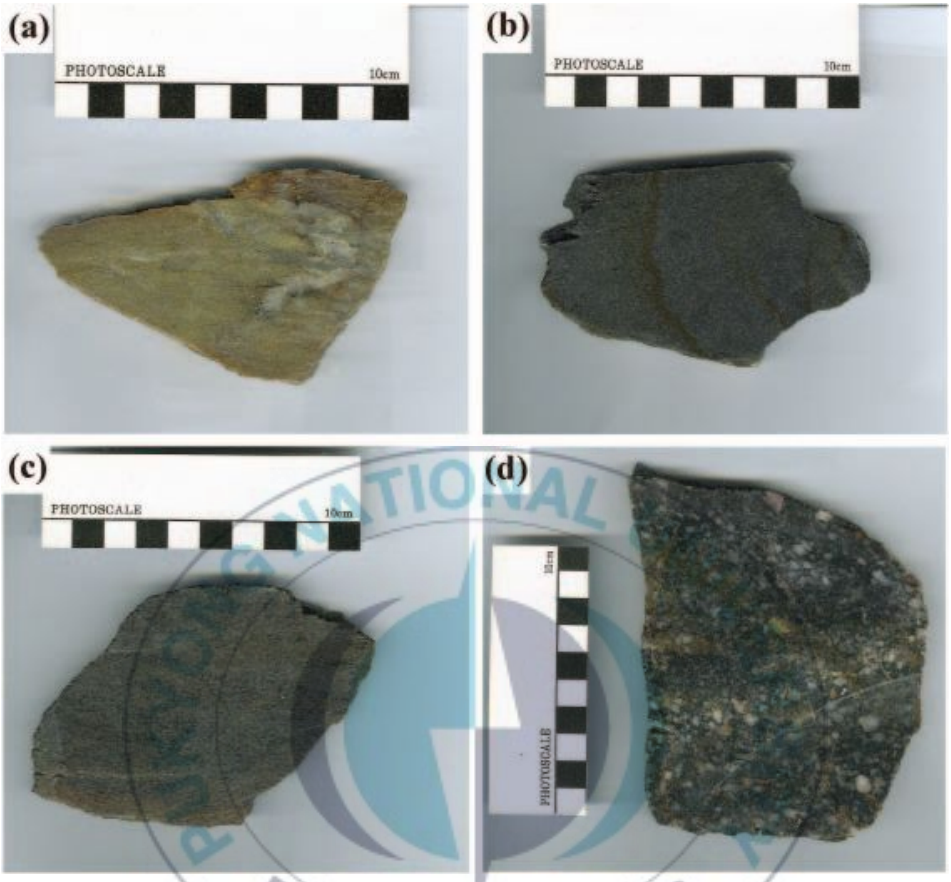

Fig. 5. Slab photographs of the metasedimentary rocks from Maldo.

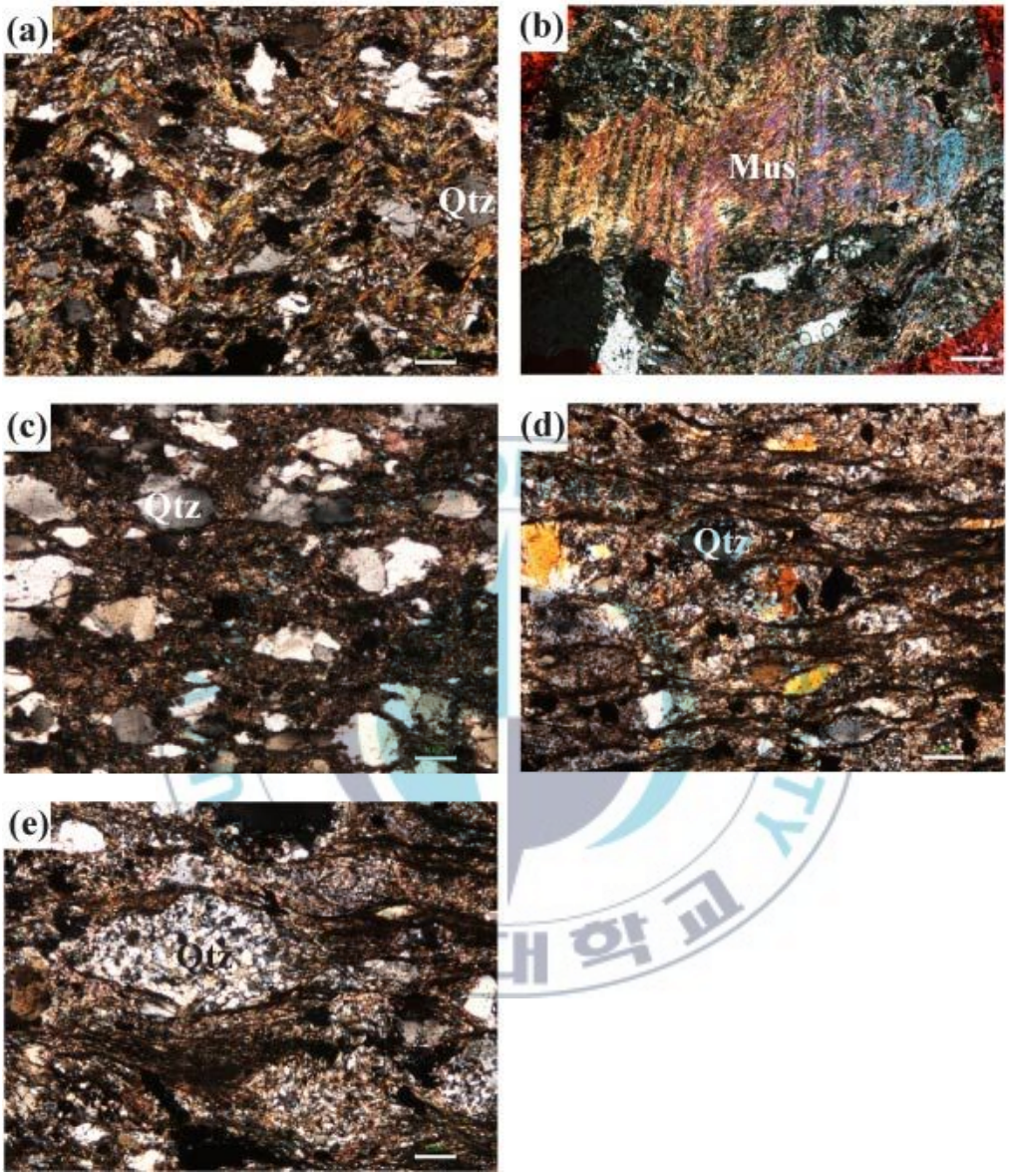

Fig. 6. Photomicrographs of the metasedimentary rocks from Maldo. (Scale bar : 100μm)

3-1-2. Metabasites

Metabasites mainly distributes in the Maldo harbor located on northern Maldo and reveals intercalated in granite or independent. Its grain is medium-coarse grain and foliation is not prominent. Because metabasites cuts metasedimentary rocks and there is no fold which is different from metasedimentary rocks metabasites intrudes after being suffered folding (Fig. 4).

Under microscope, metabasites have mineral assemblage amphibole + plagioclase + quartz + muscovite and accessory minerals are epidote, chlorite and iron bearing minerals. Amphibole's cleavage is wider because of extreme weathering and chloritization. Plagioclase is partly weathered and microgranular inclusion is being scattered (Fig. 7).

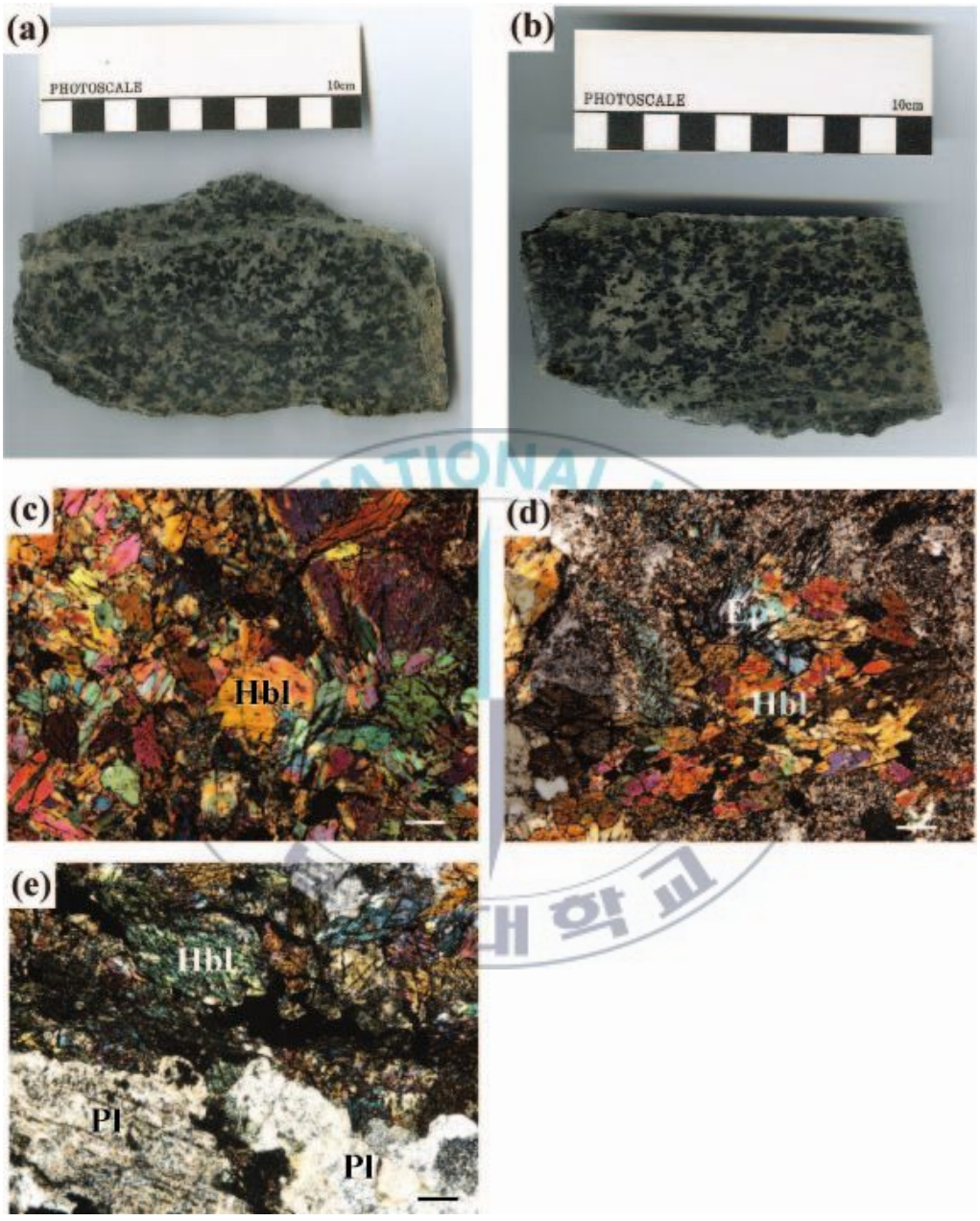

Fig. 7. Slab photographs and photomicrographs of the metabasites from Maldo. (Scale bar : 100μm)

3-1-3. Meta-granites

Meta-granites intrude metasedimentary rocks or intercalated in metabasites in Doggisum and Dando. The grain size is mainly medium-coarse grain and there is purple rounded appearance in the outcrop, it is because of oxidation of iron-bearing minerals and it has obvious foliation due to deformation (Fig. 8). Meta-granites mainly composed of quartz, K-feldspars, plagioclase and muscovite. Fluorite and carbonate minerals are a little existed. Feldspars are almost plagioclase. Besides, there are no orthoclase.

Quartz consist of polycrystalline grain and the grains of the quartz which are a little distorted show sutural texture of bond condition (Fig. 9). The grains are sometimes enlarged as well as most grains have undulatory extinction. Also then, fine quartz between the grains of the quartz are distributed after recrystallizd. Feldspars are almost plagioclase which are altered because of albitization and include microgranular inclusions. Muscovites are recrystallized to interstitial material between skeleton grain and shown curved (Fig. 9).

Fig. 8. Slab photographs of the meta-granites from Maldo.

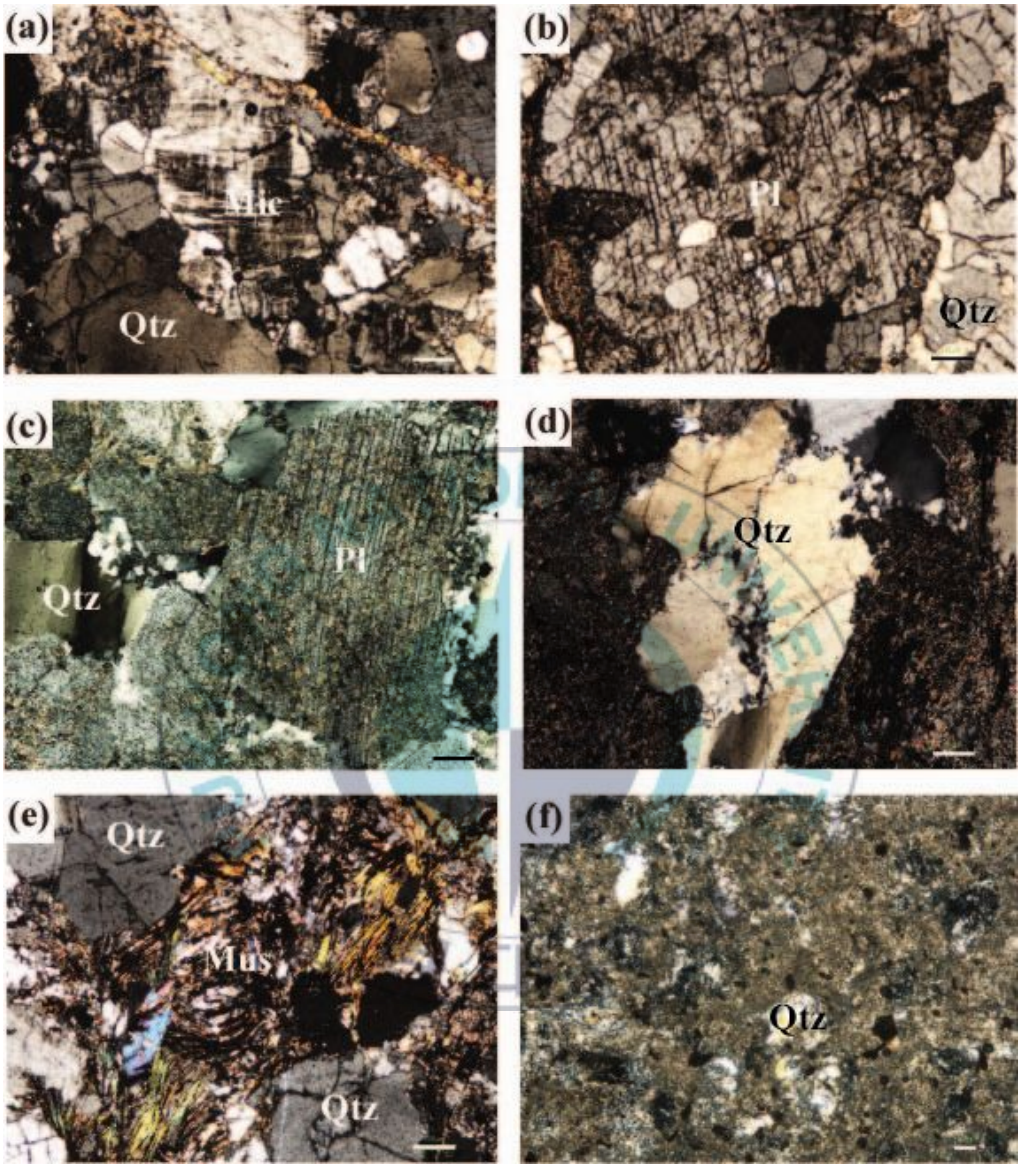

Fig. 9. Photomicrographs of the meta-granites from Maldo.
(Scale bar : 100μm)

3-2. Myeongdo

Myeongdo mainly consists of quartzite, metasedimentary formation based on altered sandstone and metabasites and meta-granites.

There are metasedimentary rocks in general, quartzite and altered sandstone in the main island. the outcrop of the dock of the main island are alternated with dark and arenaceous, grain sizes are from coarse sand to pebble (1~5mm). Sorting is poor grading and there is primary structure. Cross-bedding shows one-way direction (Fig. 10). There is high-slope cross-bedding that it means pushed appearance which is formed after sedimentation. The primary structure whose shape is preserved is assumed that it is suffered just digenesis in addition, because it consists of sandy sediment and cross-bedding, Myeongdo is sedimentary origin. Metasedimentary rocks have fold structures and microstructures. Folds are 070°-280° - this results are same as Maldo and similar folds which have unchanged formation thick in the limited areas. However, owing to a limited outcrop study, a research of a detailed geological structure is impossible.

In the dock, the outcrop by eastern seashore is 30km east and west. Both metasedimentary rocks which have pelite and metabasites alternate. Metabasites intercalate metasedimentary formation by lenticular in the middle of the outcrop (Fig. 10), metabasites and metasedimentary rocks formation intercalate each other at the upper areas. According to, two rocks intercalate mutually and are simultaneously suffered after sedimentation. Foliation is N22°~60°SE.

The pegmatite (thickness : 30cm~1m) which intrude the latter term oblique the two rocks and are simultaneously suffered with metabasites and metasedimentary formation. There are pigmatic structure in patches on the outcrop.

Outcrops located between the dock and village have metabasites and meta-granites suffered a lot. The foliation of metabasites is N55°W, 60° SW. The meta-granites are originally supposed granodiorite and they are fairly gneiss. Enclave included to meta-granites are quite enlarged by foliation (N10°W, 44°SE). There are violet minerals supposed as iron-bearing minerals on the outcrops.

The essential minerals in the meta-granites are quartz, feldspars and muscovites. Feldspars are almost plagioclase there is no orthoclase on the thin section so granite is tonalite.

Under microscope, metasedimentary rocks consist of quartz and muscovite as well as a little feldspars and iron-bearing minerals. On the thin section, minerals have the same direction. quartz are almost polycrystalline quartz when compared with monocrystalline quartz and superior to undulatory extinction. Moreover, the grains are a little enlarged. Muscovite appear matrix shape of metasedimentary rocks with feldspar group and there are sometimes muscovite recrystallized (Fig. 15e). Metabasites constitute the grains of amphiboles, plagioclase, quartz and muscovite. Accessory minerals are chlorite, epidote and iron-bearing minerals. The amphiboles and muscovites are suffered chloritization. Felspars are almost plagioclase terribly altered because of albitization. There are microgranular inclusions inside felspars. meta-granites consist

of quartz, muscovite and amphibole mainly and a little chlorite and iron-bearing minerals. The quartz have clean surface, undulatory extinction, anhedral and superior to polycrystalline quartz. The amphibole and muscovite are almost chloritization. The iron-bearing minerals include pyrite and chalcopyrite which are secondary oxidized mineral with ilmenite (Fig. 13).

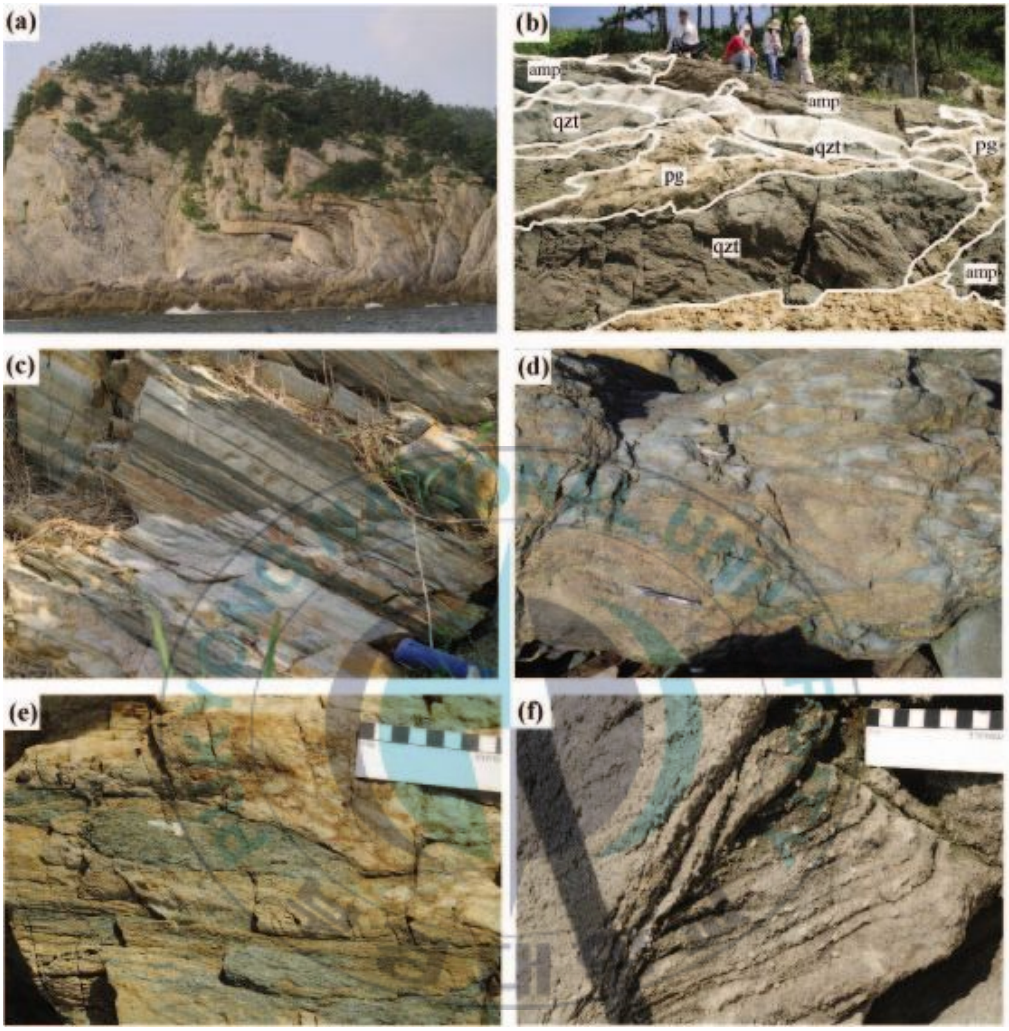

Fig. 10. Outcrop photographs of the metamorphic rocks Myeongdo.

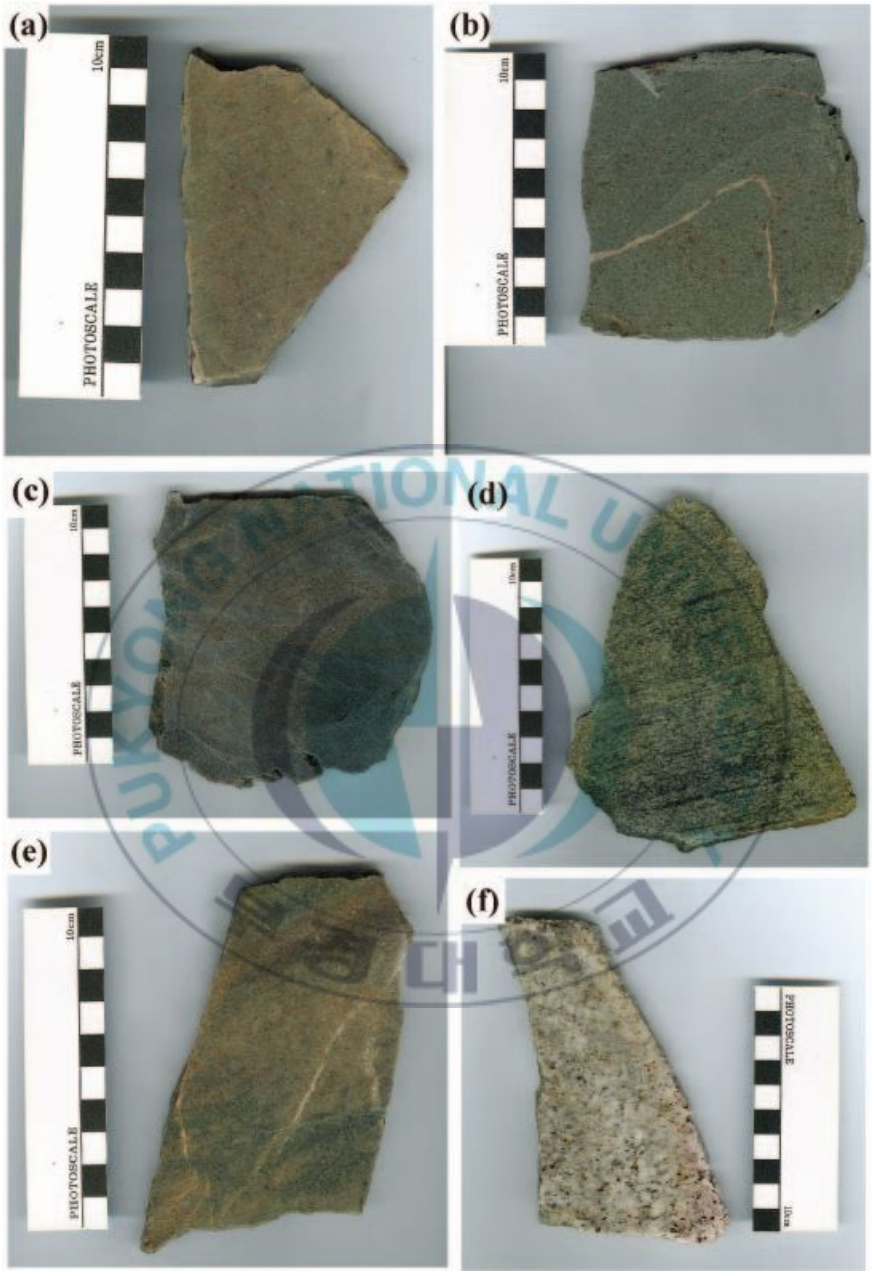

Fig. 11. Slab photographs of the metasedimentary rocks from Myeongdo. (a, b & c) metasedimentary rocks, (d. e & f) meta-granites.

Fig. 12. Slab photographs of the metabasites from Myeongdo.

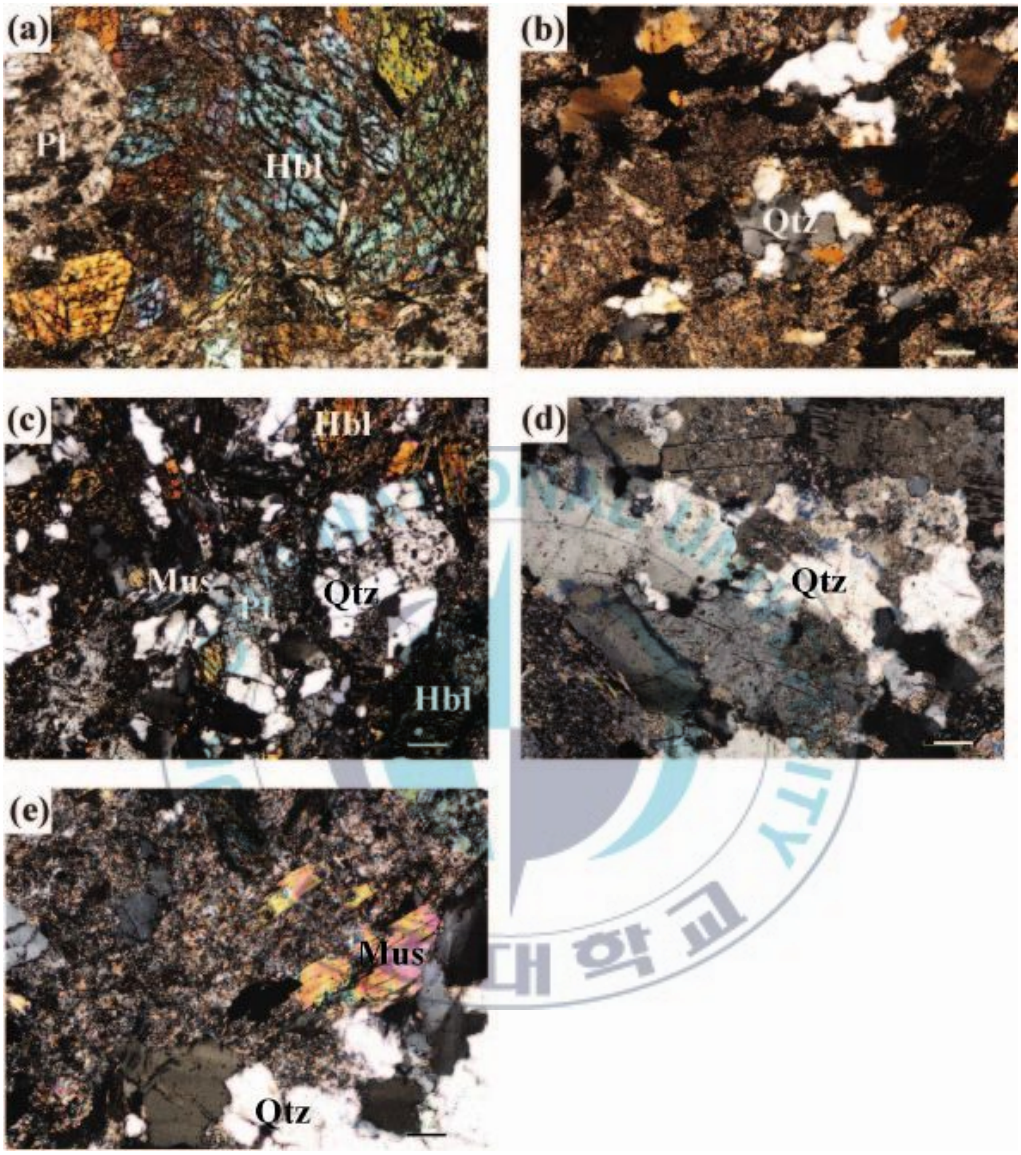

Fig. 13. Photomicrographs of the (a) metabasites (b, c & d) meta-granites (e) metasedimentary rocks from Myeongdo.
(Scale bar : 100μm)

4. Geological structure

Geological structures of the Okcheon metamorphic belt consider they are suffered several times (Chang et al,. 1998; Cluzel et al., 1991; Kang et al., 1993; Koh and Kim, 1995; Kang and Ryoo, 1997; Kang, 2001). To examine the history of the geotectonics of the Okcheon metamorphic belt, they are classified according to step by step instructions.

Metasedimentary rocks distribute to E-W direction from Maldo - Bonongdo - Myeongdo - Kwangdaedo - Bangchungdo - Sohoenggyeongdo - Hoenggyeongdo to Keido. This formations have the former isoclinal folds whose regional foliation is axial plane and the latter open folds that make the former isoclinal re-folding. The latter open folds are made by secondary folding and constitute a large scale folding structure having 070°-280° axis. The north islands of Gogunsan islands mentioned arrange the same direction with the axis direction of this folding structure. The minimum three times folding and a variety of geological structures because of those appear the limited outcrop scale, and moreover both parallel folds and similar folds depending on a property of matter. There is thrust duplex structure optionally at a portion quartzite formation of Maldo (Kee and Hwang, 2007) (Fig. 16).

4-1. Primary Fold (D1)

Primary folds of Maldo and Myeongdo are observed at the quartzite

formation located on right lower part of figure 14(a) and appear the limb of secondary folds. This primary folds are assumed that they are associated with tectonic movement formed regional foliation (Kee and Hwang, 2007).

4-2. Secondary fold (D2)

Fold sections in the study area are most secondary folds yielded upright open folds having a vertical axial plane. The secondary folds of this point have integrated vergence to the north direction. Anticline are presumed to be located on the upper area of that. Quartzite show parallel fold. Story of dark gray phyllite formation intercalated between quartzite formation have very thick hinges but limb show similar fold (Kee and Hwang, 2007).

4-3. Third fold (D3)

The third folds recoded the last folding are restrictively observed at quartzite formation. Figure 14(b) is a picture of the third folds that shows a small scale open fold formed a wrinkled shape. Axial planes of the folds are perpendicular and folds axis which are 013°-193° are assumed that the secondary fold are oblique as well as the distances between axises appear narrow less than 1m relatively (Kee and Hwang, 2007).

4-4. Thrust duplex

Duplex defines a bedrock divided a fault. In fact, means geological structure which is yielded horses having imbricate facies (Fig. 17). In the outcrops of Maldo, thrust duplex structure related with the secondary folding shows up some quartzite formation optionally and the portions of thrust folds present folded thrust curved itself (Fig. 16).

Thrust duplex structure is a geological structure which is formed because of flexureal slip mechanism happened in accordance with both upper and lower the boundary surface of sheets, and means imbricate facies repetitively distributed horses in order of precedence divided with thrust fault movement. Weaker phyllite formation compared with quartzite formation is generated more inner transformation than the thrust structure while suffering compressed transformation.

Folded thrust implies that the secondary folding is happened, and it is transformed due to a folding after fault plane. However, the thrust faust next to Maldo's shore outcrops shows up transport direction which is almost same as the axial plane of the secondary fold structure. Also, both the thrust fault and the secondary fold structure indicate that are formed at the almost same time under a serial compressed transformation domain (Kee and Hwang, 2007).

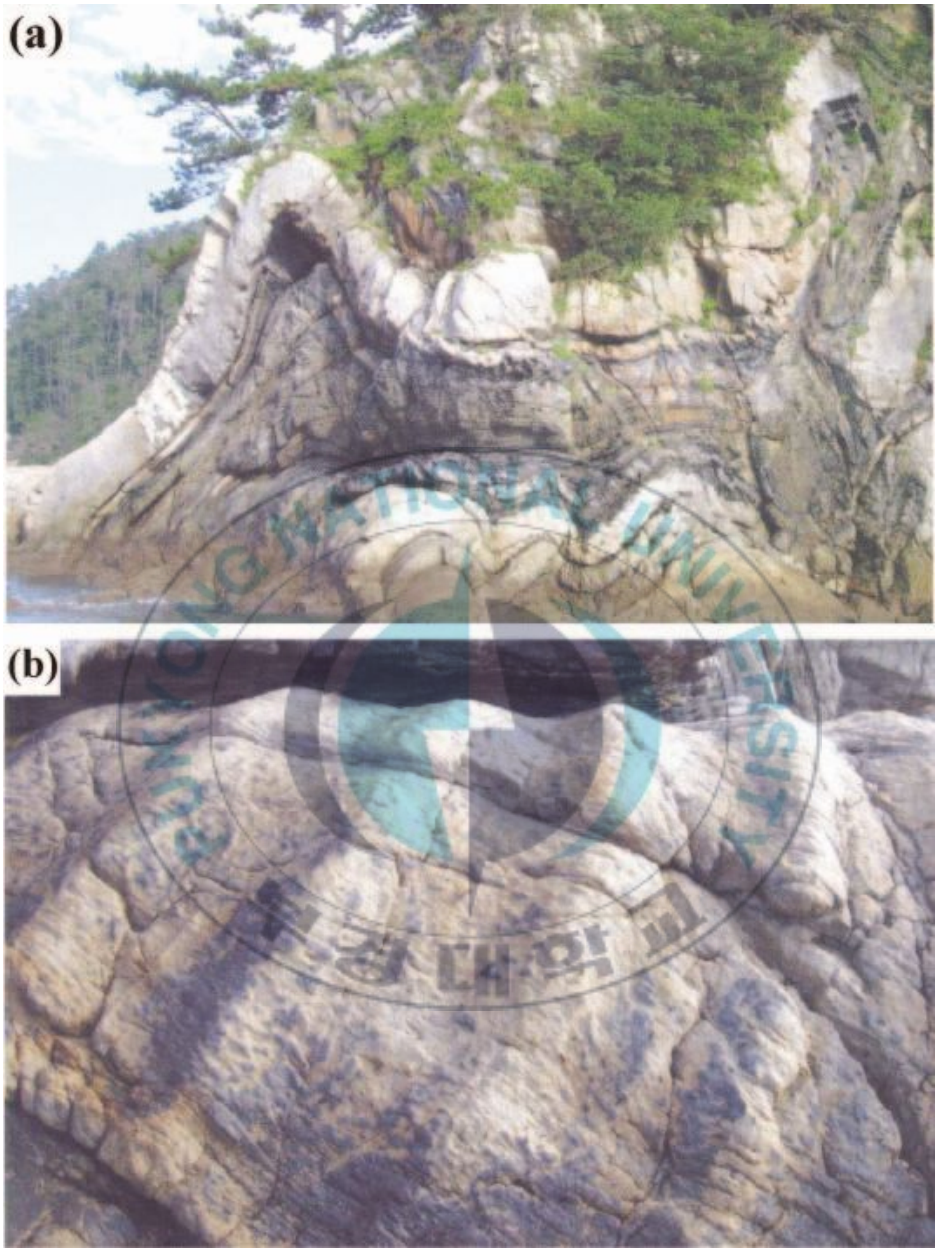

Fig. 14. Photographs of the metasedimentary rocks of Maldo showing folded structures (a) D1 & D2, (b) D3 deformations (Kee and Hwang, 2007).

Fig. 15. Photographs of D2 fold from Maldo.

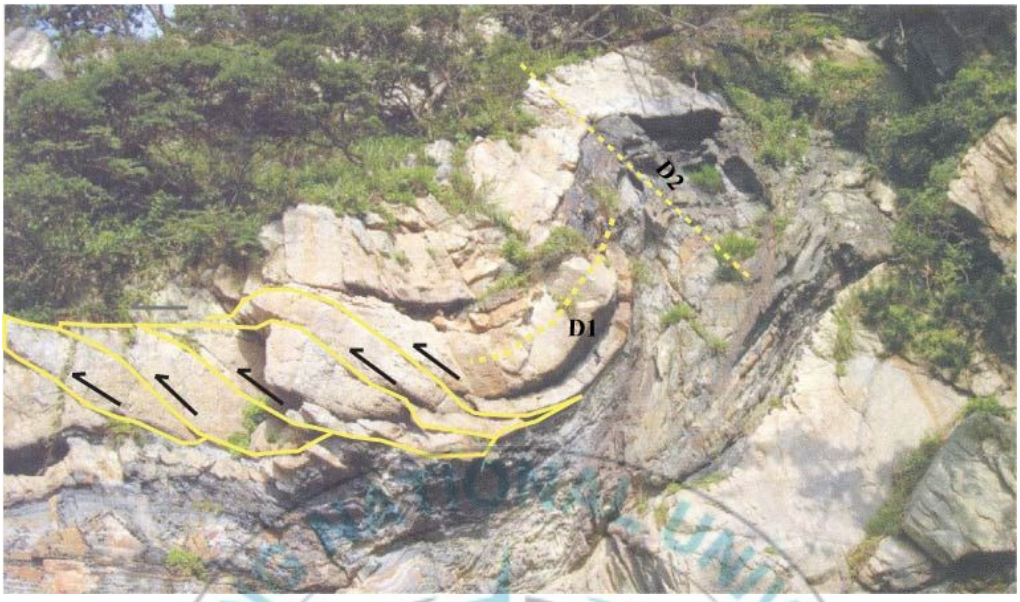

Fig. 16. Photograph of thrust duplex from Maldo.

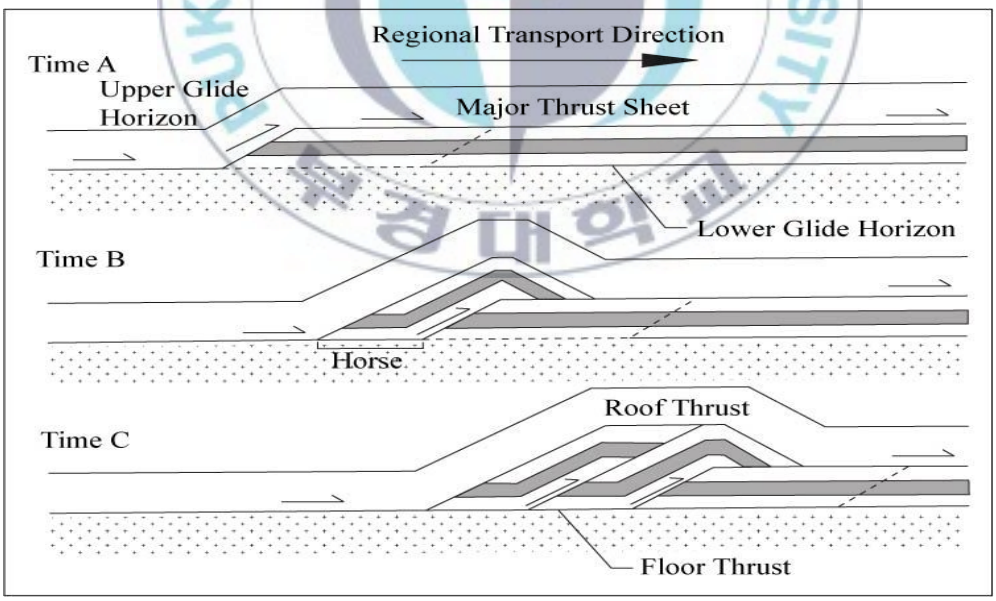

Fig. 17. The model of advancement process of duplex structure from Davis & Reynolds (1996).

5. Geochemistry

5-1. Method

Major element data were obtained using a SHIMADZU XRF-1700 of X-ray Fluorescence spectrometer (XRF) at the Cooperative Laboratory Center of Pukyong National University. The analytical conditions were 70mA in beam current and 40kV in accelerating voltage. Average values were calculated from three measurements for each sample. Major element abundances for the studied samples are reported in Table 1~4.

Trace and rare earth elements were obtained using a Thermo Elemental X-5 of inductively-coupled plasma mass spectrometer (ICP-MS) at Korea Basic Science Institute in Daeieon. Trace and rare earth elements abundance are reported in Table 5~7.

5-2. Major elements

5-2-1. Metasedimentary rocks

Na_2O average contents in study area is 0.21wt%, 3.56wt%, respectively and K_2O average contents which is 5.97wt% and 3.71wt% is higher than average contents of clastic sediment rocks (Table 1). The origin of Na_2O is feldspars, particularly, plagioclase comes from digenesis of clay minerals (Lee and Lee, 1988). K_2O is major elements

of K-feldspar, micas, illite. Na and K contents are easily moved during weathering. Because the former becomes leaching, the latter becomes absorption (Rankama and Sahama, 1950), most shale and slate have higher K than Na contents. K_2O contents in Maldo is higher than Na_2O contents in Myeongdo in the K_2O-Na_2O correlation (Fig. 18).

Fe_2O_3/K_2O ratio defines mineralogical stability. The most stable minerals is quartz, K-feldspar and muscovite in the low-T/Low-P environments. K-feldspar and muscovite have abundant K and little Fe contents. In the contrast, unstable biotite and amphiboles have abundant Fe and Mg contents. Therefore, stable minerals show low Fe_2O_3/K_2O ratio but unstable minerals show high Fe_2O_3/K_2O ratio (Table 1). If those minerals plot in Sand Class System, because Fe_2O_3/K_2O ratio is very high, it is discriminated as Fe-shale or Fe-sand (Go and Shin, 1995). In this study, metasedimentary rocks are plotting wacke mainly, litharenite, Fe-shale and arkose (Fig. 19).

In the tectonic discrimination based on SiO_2-K_2O/Na_2O, metasedimentary rocks in Maldo and Myeongdo are mainly plotting in passive margin (PM) and one of Maldo sample is plotting in active continental margin (ACM). Sediments classified as the PM comes from near part PM (Fig. 20) (Roser and Korsch, 1986).

Table 1. Representative major element compositions (wt%) of the metasedimentary rocks in the study area.

Sample	mm-4a	mm-8-1	mm-12	mm-21	mm-22	mm-24
SiO_2	68.64	61.27	71.73	70.2	40.24	73.76
Al_2O_3	16.12	8.13	15.64	15.96	12.12	14.37
TiO_2	0.53	0.52	0.33	0.26	3.28	0.25
Fe_2O_3	6.57	3.61	4.45	1.9	13.56	1.52
MnO	0.01	0.24	0.01	0.03	0.17	0.02
MgO	0.36	3.77	0.29	0.78	4.11	0.58
CaO	0.12	6.4	0.13	1.03	6.06	0.55
Na_2O	0.04	0.56	0.02	4.33	0.94	4.81
K_2O	4.85	2.35	4.73	2.83	2.39	2.2
P_2O_5	0.06	0.1	0.07	0.08	0.51	0.06
LOI	2.25	12.74	2.15	2.59	16.05	1.33
Total	99.55	99.7	99.55	99.98	99.44	99.42

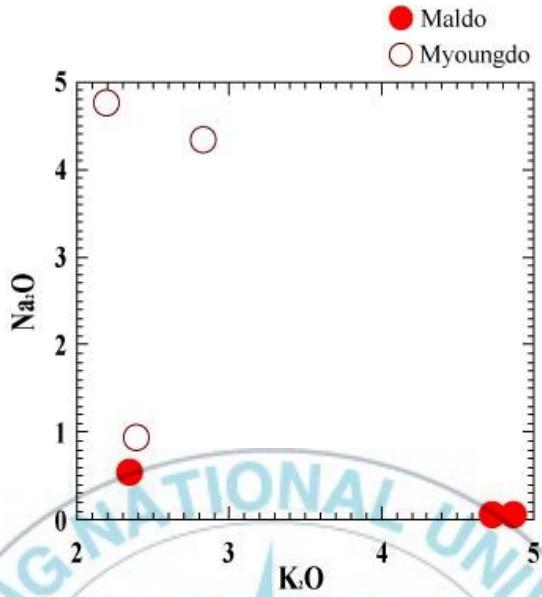

Fig. 18. Variations of Na_2O and K_2O content of the metasedimentary rocks in the study area.

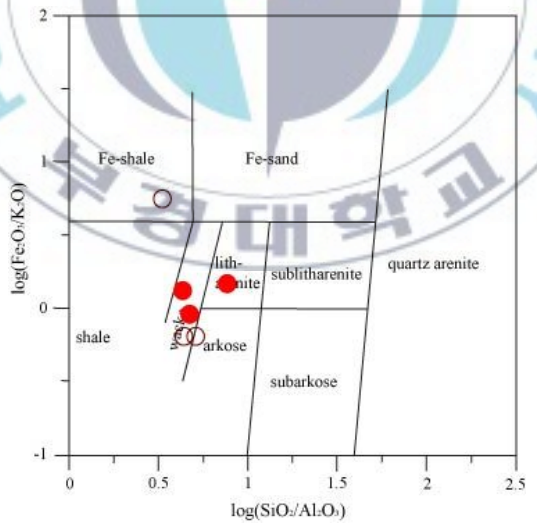

Fig. 19. Chemical classification diagram of sedimentary source materials (Herron, 1988) for the metasedimentary rocks from the study area.

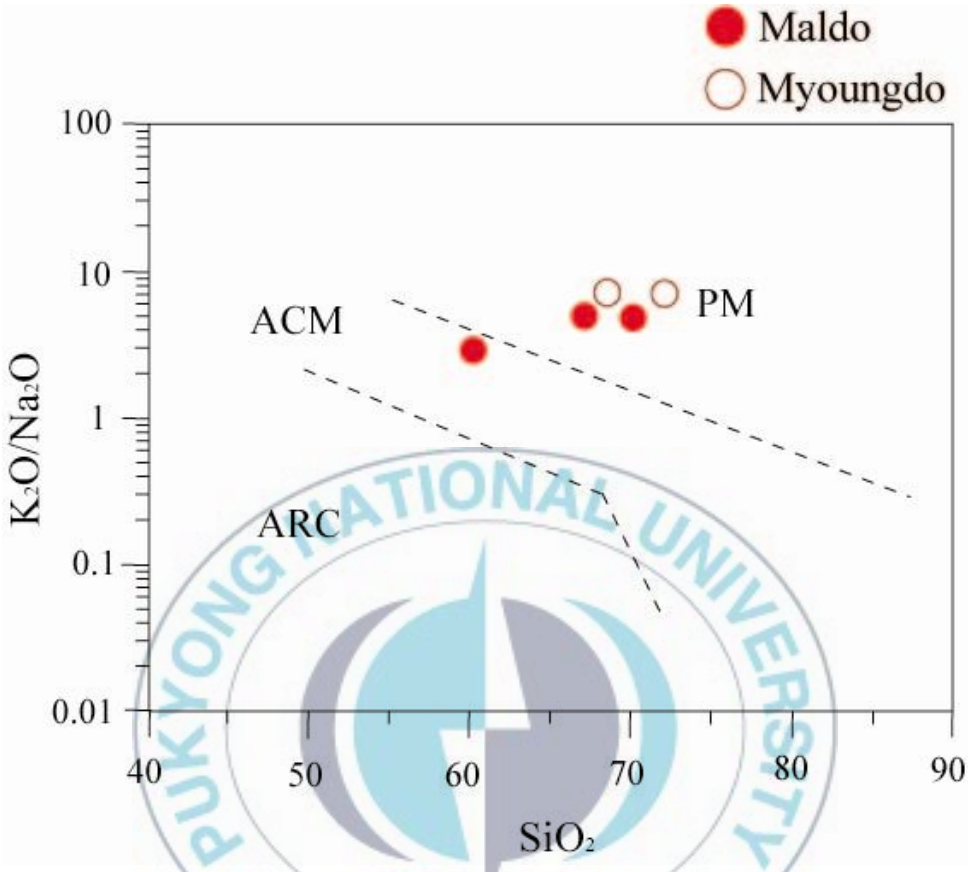

Fig. 20. SiO_2–K_2O/Na_2O discrimination diagram from the metasedimentary rocks in the study area. PM: passive continental margin, ACM: active continental margin, ARC: oceanic island arc (after Roser and Korsch, 1986).

5-2-2. Meta-granites

The content of SiO_2 in the analyzed plutonic rocks was 55.39~89.60wt% (Table 2, 3). Plotting on a total alkali-silica (TAS) diagram (Irvine and Baragar, 1971), the most analyzed rocks were included in sub-alkaline series (Fig. 21(a)). Illustrating chemical compositions of the analyzed rocks on the AFM triangular diagram (Irvine and Baragar, 1971) that distinguishes original magma series, the most rocks included in calc-alkaline field as well as on boundary of tholeiitic and calc-alkaline field (Fig. 21(b)). The major oxides analyzed for understanding the difference of magma process of each rock are illustrated on the Harker variation diagram of SiO_2 increase (Fig. 22). According to the analyzed results, generally as the content of SiO_2 increase, that is, as differentiation proceeds, the contents of major elements of each rock show a comparably systematic increase following general trends of magma differentiation by crystal differentiation.

The decrease of Al_2O_3 shows that plagioclase was crystallized during the process of differentiation, and the decrease of TiO_2, Fe_2O_3 and MnO contents reveals that mafic minerals were crystallized during the process of differentiation. And the content of K_2O showing a relative increase pattern the fact that alkali feldspars, which contains much K that is crystallized during magma differentiation (Fig. 22).

According to the results of illustrating on the ACF triangular diagram, all meta-granites were included in the domain of S-type granites (Fig. 24).

Table 2. Representative major element compositions (wt%) of the meta-granites from the Maldo.

Sample	mm-4	mm-5-1	mm-6	mm-6 (k-Ar)	mm6a	mm-6c	mm-7	mm-8	mm-8-1
SiO_2	88.60	73.77	61.62	55.96	55.97	70.02	62.78	71.98	55.39
Al_2O_3	2.19	14.61	15.84	13.30	19.37	14.94	17.23	14.84	20.29
TiO_2	0.06	0.14	0.55	1.34	0.60	0.14	0.58	0.35	0.81
Fe_2O_3	1.21	1.07	6.51	7.51	6.04	1.13	4.08	3.56	4.95
MnO	0.10	0.03	0.19	0.14	0.13	0.04	0.06	0.03	0.07
MgO	1.72	0.15	0.93	2.30	1.35	0.51	1.77	0.35	1.83
CaO	2.67	0.16	1.02	4.15	1.86	1.48	1.79	0.23	1.86
Na_2O	0.01	2.88	2.61	3.18	4.81	2.78	3.27	3.67	3.29
K_2O	0.54	6.24	5.27	2.54	3.57	5.81	2.97	2.97	4.68
P_2O_5	0.01	0.05	0.19	0.18	0.18	0.25	0.20	0.14	0.18
LOI	4.40	0.91	4.51	9.27	5.74	2.60	4.42	1.94	5.86
Total	101.50	99.99	99.23	99.87	99.62	99.70	99.15	100.08	99.22

Table 3. Representative major element compositions (wt%) of the meta-granites from the Myeongdo.

Sample	mm-21 (GPS139)	mm-22	mm-24 -opg-a	mm-25
SiO_2	70.82	75.33	67.84	67.05
Al_2O_3	15.61	14.11	16.23	14.74
TiO_2	0.14	0.07	0.03	0.42
Fe_2O_3	1.39	0.65	0.91	2.87
MnO	0.03	0.03	0.04	0.03
MgO	0.49	0.51	1.59	1.62
CaO	1.35	0.90	1.59	1.87
Na_2O	5.18	6.83	5.56	4.67
K_2O	2.50	0.94	2.57	2.29
P_2O_5	0.03	0.01	0.00	0.11
LOI	2.11	0.37	3.42	3.76
Total	99.65	99.75	99.78	99.45

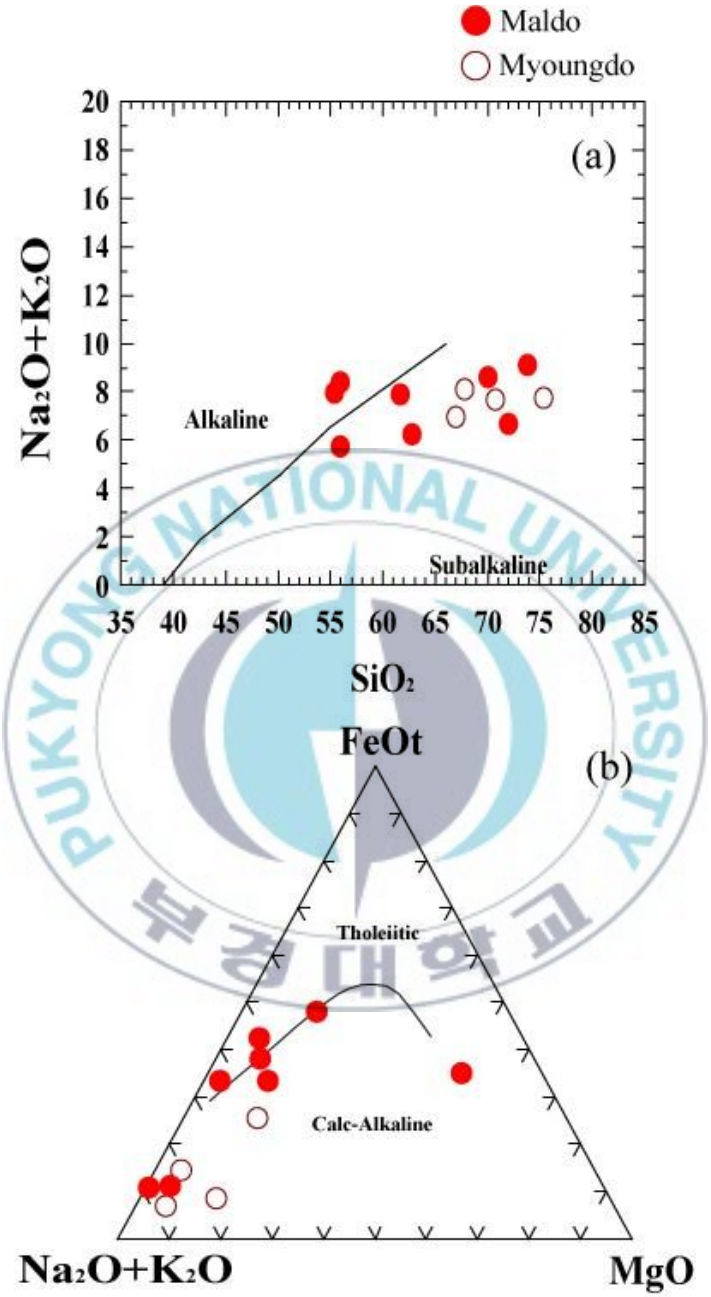

Fig. 21. (a) Total-alkali versus silica (TAS) and (b) ternary AFM (Irvine and Baragar, 1971) diagrams for the meta-granites in the study area.

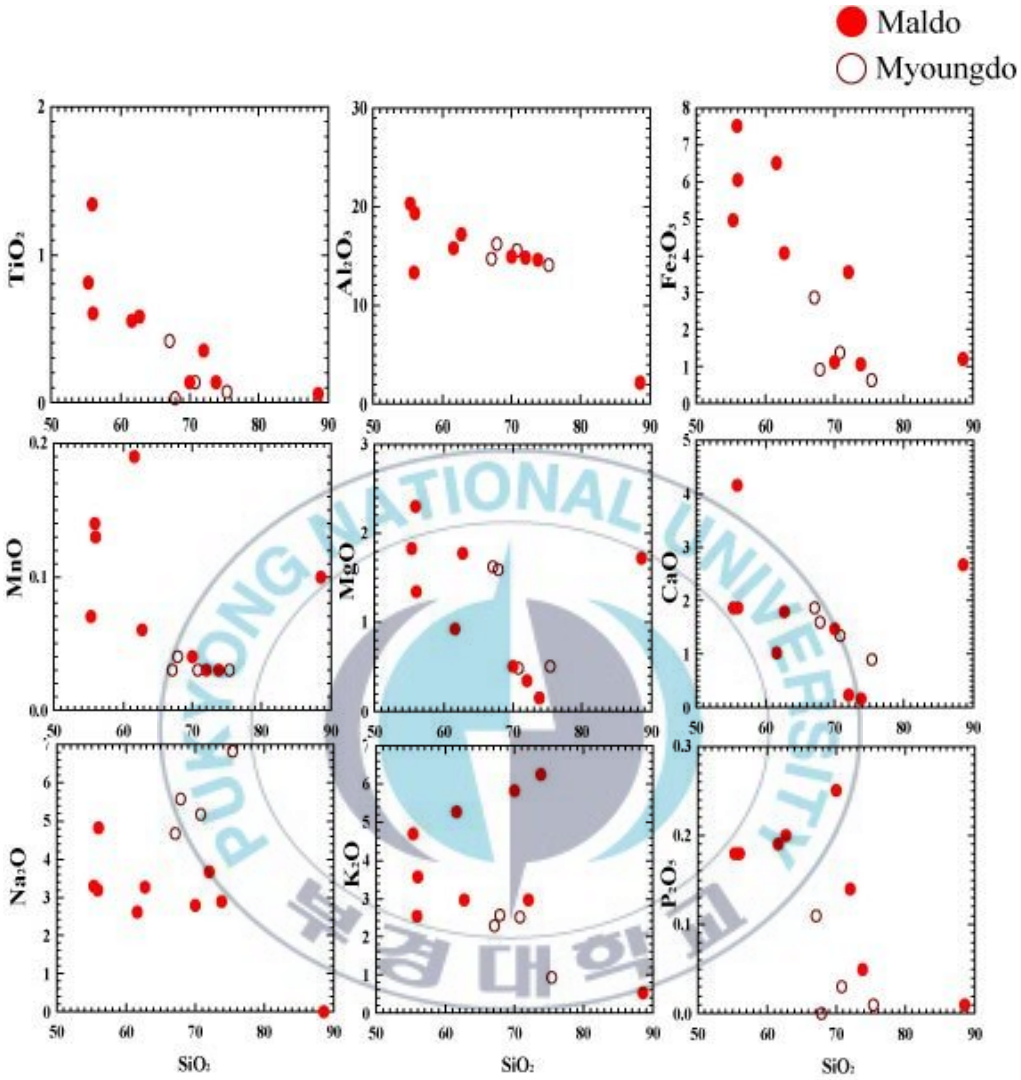

Fig. 22. Harker diagrams for the meta-granites in the study area.

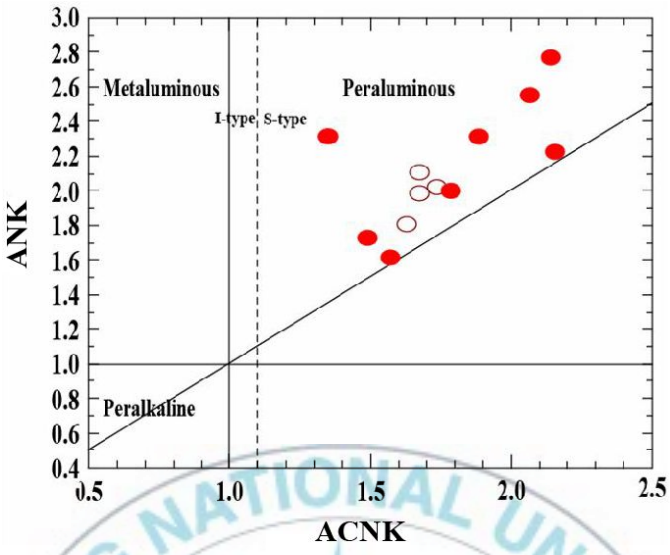

Fig. 23. ACNK vs. ANK (molar $Al_2O_3/(CaO+Na_2O+K_2O)$ vs. $Al_2O_3/(Na_2O+K_2O)$) diagram (Mauriar and Piccoli, 1989) for the meta-granites in study area. Symbols are same as in Fig. 24.

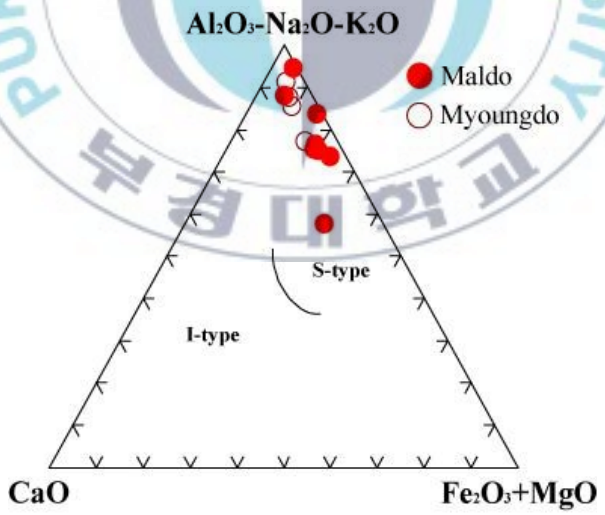

Fig. 24. ACF ternary diagram (molar ratio, A: $Al_2O_3-Na_2O-K_2O$, C : CaO, F : Fe_2O_3+MgO) for the meta-granites in the study area.

5-2-3. Metabasites

The results of metabasites analyses of the study area are listed in Table 4.

The results plotted on Niggle's mg-c diagram to assume the origin of metabasites show igneous metabasites (Fig. 25). Most samples are plotted on subalkaline series in the Total Alkali-Silica (TAS) diagram (Irvine and Baragar, 1971) (Fig. 26(a)).

Table 4. Representative major element compositions (wt%) of metabasites from Maldo and Myeongdo.

Sample	mm-9	mm-10	mm-25	mm-26	mm-27
SiO_2	52.39	52.42	49.28	48.86	56.27
Al_2O_3	17.06	15.99	11.92	12.13	16.11
TiO_2	0.48	1.01	0.44	0.5	0.8
Fe_2O_3	7.97	9.84	9.71	9.6	7.34
MnO	0.15	0.14	0.15	0.14	0.1
MgO	6	6.2	9.93	12.76	4.45
CaO	7.15	6.43	8.66	8.79	5.62
Na_2O	3.82	3.7	2.08	1.89	3.94
K_2O	2.08	1.7	1.63	1.51	1.82
P_2O_5	0.06	0.08	0.03	0.01	0.28
LOI	2.35	2.58	5.71	2.99	2.65
Total	99.51	100.1	99.53	99.18	99.38

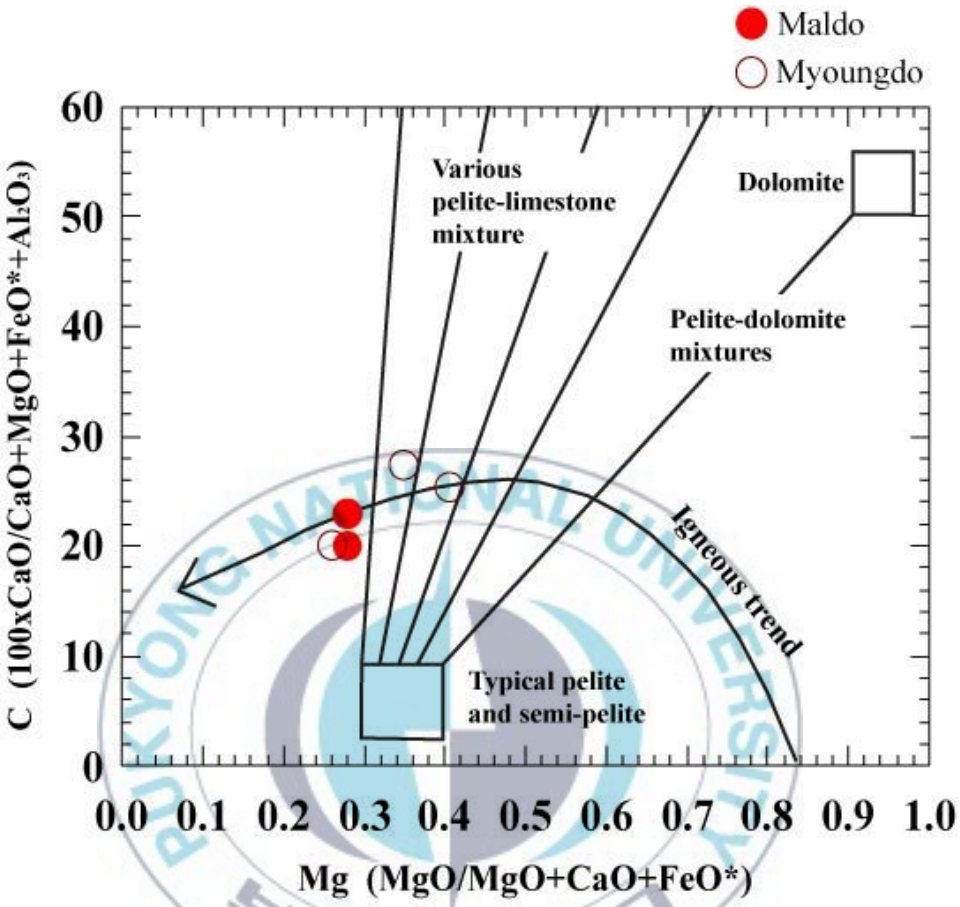

Fig. 25. Niggli mg-c plot of metabasites from the study area slightly modified after Leake (1964).

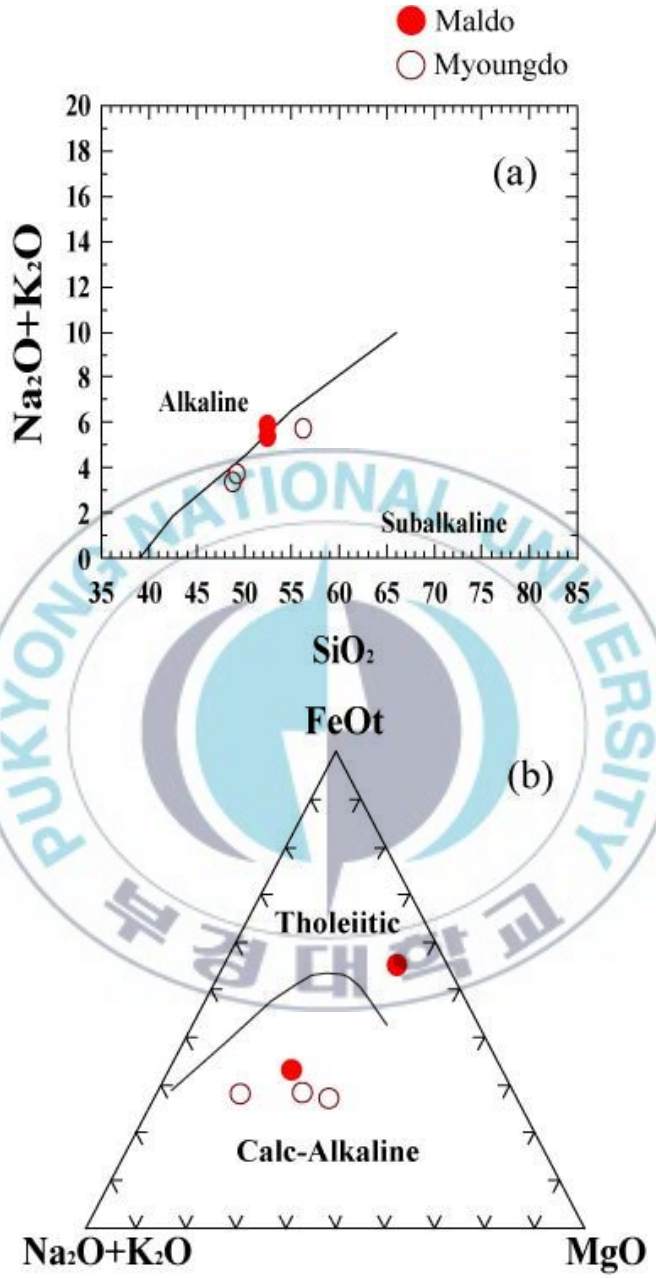

Fig. 26 (a) Total-alkali versus silica (TAS) and (b) ternary AFM diagrams (Irvine and Baragar, 1971) for the metabasites in the study area.

5-3. Trace and rare earth elements

The result of trace and rare earth elements of meta-granites and metabasites in the study area is listed in Table 5~7.

Figure 27 shows patterns of trace and elements generalized by C1 Chondrite contents (Sun & McDonough, 1989). The results show that an overall tendency shows similar patterns and Nb (-) anomaly. This obvious Nb (-) anomaly is a distinguished feature and comes from subduction environment or lower material of back-arc basin.

Meta-granites distinguished in Maldo and Myeongdo belong to meta-granites of island arc type and all metabasites are plotted in subduction environments (Fig. 28). It means that metabasites are formed at subduction boundary because of basalt and its differentiates (Fig. 29). Figure 30 shows that metabasites erupts from calc-alkali basalt.

Table 5. Trace element and REE compositions (ppm) of meta-granites from Maldo.

Sample	mm-4	mm-5-1	mm-6	mm-6 (K-Ar)	mm-6a	mm-6c	mm-7	mm-8	mm-8-1
Ba	265.5	683.4	2812.7	769.7	1401.8	1644.8	503.5	757	677.1
Sr	93.3	128.1	188.3	128.5	245.7	237.9	197.2	84.6	216
Cr	453.44	0.75	82.86	235.19	92.23	0.66	3.28	7.81	69.7
Co	9.58	31.9	4.16	28.47	5.21	59.13	27.85	61.38	8.62
Ni	13.78	0.3	4.02	50.99	5.31	1.08	9.9	5.48	10.59
Cu	2.71	0.03	5.69	49.05	9.18	0.84	21.24	4.03	11.89
Zn	32.68	13.09	75.71	73.3	69.04	16.87	70.33	44.32	52.61
Li	1.6	2.2	5.7	15.6	13.2	3.3	52.8	8.2	69.8
Sc	3.05	5.31	20.58	26.82	17.55	3.78	13.4	8.03	14.11
V	16.3	3.2	12	191.2	11.4	2.8	17.9	14	23.7
Zr	19.7	109.1	238.3	111.4	267.8	22.6	140.6	127.3	212.7
Rb	20.26	141.18	116.63	76.26	104.82	101.39	108.88	97.62	178.19
Y	4.4	15.85	78.25	22.12	62.98	11.33	24.23	19.51	28.02
Nb	1.35	2.54	23.32	22.29	21.38	4.49	14.19	5.93	14.12
Cs	0.84	1.58	5.75	2.09	4.21	1.4	8.09	2.48	5.47
La	13.07	60.26	99.38	17.52	34.53	15.46	137.76	81.77	149.28
Ce	24.2	124.97	200.27	36.45	74.63	32.25	267.05	171.82	285.66
Pr	2.54	13.53	22.46	4.42	9.35	3.94	28.89	19.49	31.58
Nd	9.06	46.33	82.73	18.21	37.7	16.25	105.29	70.46	116.06
Sm	1.53	9.12	13.54	4.02	8	3.88	14.81	11.47	17.4
Eu	0.34	1	5.16	1.24	5.33	2.74	4.59	1.88	5.45
Gd	1.06	5.86	10.57	4	8.27	3.51	9.11	6.57	11.09
Tb	0.16	0.76	1.83	0.68	1.52	0.55	1.15	0.84	1.38
Dy	0.88	3.57	13.37	4.52	11.37	2.91	5.97	4.53	6.97
Ho	0.15	0.62	3.4	0.97	2.73	0.44	1.06	0.73	1.23
Er	0.45	1.69	11.72	2.84	9.33	1.07	2.79	1.78	3.17
Tm	0.06	0.24	1.88	0.42	1.46	0.12	0.39	0.21	0.4
Yb	0.45	1.55	13.52	2.78	10.89	0.81	2.67	1.25	2.9
Lu	0.06	0.21	2.15	0.41	1.74	0.13	0.42	0.15	0.41
Hf	0.54	2.5	3.98	3.08	5.21	0.59	3.07	2.72	3.4
Ta	0.65	1.04	6.68	8.37	6.67	2.48	4.9	2.14	2.8
Pb	3.14	32.23	17.87	2.95	36.03	33	12.44	36.51	18.73
Th	2.25	30.86	19.14	5.07	6.3	1.43	16.22	18.16	21.84
U	0.2	1.99	1.98	0.85	3.09	0.87	2.78	3.81	2.95

Table 6. Trace element and REE compositions (ppm) of meta-granites from Myeongdo.

Sample	mm-21(GSP139)	mm-22	mm-24(opg-a)	mm-25
Ba	720.6	340.5	842.9	580.2
Sr	295.1	176.1	191.6	206.9
Cr	193.60	0.81	5.12	3.90
Co	1.66	33.33	25.96	32.58
Ni	3.29	2.00	9.13	7.85
Cu	6.96	4.13	17.72	7.16
Zn	24.33	10.48	6.45	37.27
Li	5.9	5.1	10.7	6.5
Sc	3.48	3.64	2.93	5.87
V	6.2	2.7	1.9	22.2
Zr	48.2	51.4	29.1	158.0
Rb	88.90	32.00	106.74	89.19
Y	3.53	5.19	6.02	13.25
Nb	6.93	1.71	0.91	8.60
Cs	3.34	1.18	3.02	3.59
La	7.58	20.31	8.95	68.88
Ce	14.72	39.76	17.06	129.53
Pr	1.62	4.39	1.78	13.59
Nd	5.90	15.73	6.03	46.24
Sm	1.19	3.37	1.39	7.92
Eu	0.37	0.63	0.28	1.45
Gd	0.89	2.18	1.22	5.28
Tb	0.13	0.30	0.20	0.72
Dy	0.80	1.36	1.16	3.63
Ho	0.13	0.23	0.23	0.57
Er	0.38	0.57	0.72	1.46
Tm	0.05	0.08	0.12	0.18
Yb	0.36	0.59	0.78	1.12
Lu	0.05	0.09	0.12	0.16
Hf	1.37	1.47	1.58	3.76
Ta	0.95	0.71	1.07	2.36
Pb	9.79	6.08	4.28	6.65
Th	2.19	20.83	5.31	21.72
U	0.51	3.81	2.11	1.71

Table 7. Trace element and REE compositions (ppm) of meta-granites from Maldo and Myeongdo.

Sample	mm-9	mm-10	mm-25	mm-26	mm-27
Ba	437.1	425.3	1022.6	475.6	551.7
Sr	387.7	422.7	549.2	180.8	537.8
Cr	66.86	112.95	239.42	675.22	126.76
Co	35.35	33.15	57.22	61.47	30.80
Ni	21.85	26.33	89.08	174.18	49.88
Cu	1.47	3.08	76.07	74.70	54.06
Zn	75.11	92.29	71.40	59.93	67.48
Li	13.4	34.1	22.5	24.5	18.4
Sc	24.29	26.07	37.60	36.22	16.68
V	118.6	143.2	155.4	146.5	109.8
Zr	26.4	46.5	18.2	13.0	24.3
Rb	77.48	62.60	60.50	52.42	56.57
Y	10.36	17.30	8.98	8.81	15.27
Nb	2.71	4.97	1.44	0.88	7.43
Cs	3.05	2.43	26.26	2.50	6.13
La	6.90	10.48	5.68	3.19	21.14
Ce	13.94	21.47	13.80	6.98	48.84
Pr	1.74	2.87	1.90	1.08	6.48
Nd	7.18	12.30	8.33	5.22	27.04
Sm	1.77	3.00	2.21	1.49	5.35
Eu	0.98	1.27	0.68	0.60	1.46
Gd	1.85	3.08	1.94	1.71	4.19
Tb	0.31	0.51	0.34	0.28	0.57
Dy	2.14	3.35	2.07	1.82	3.38
Ho	0.44	0.69	0.39	0.37	0.64
Er	1.24	2.01	1.07	1.06	1.71
Tm	0.18	0.28	0.16	0.14	0.24
Yb	1.22	1.89	1.03	0.99	1.52
Lu	0.18	0.27	0.15	0.14	0.22
Hf	0.91	1.49	1.11	0.70	1.09
Ta	1.23	2.26	0.58	0.51	3.47
Pb	6.61	3.88	4.99	3.45	5.86
Th	2.14	2.17	2.70	0.56	3.83
U	0.34	1.02	0.27	0.18	0.68

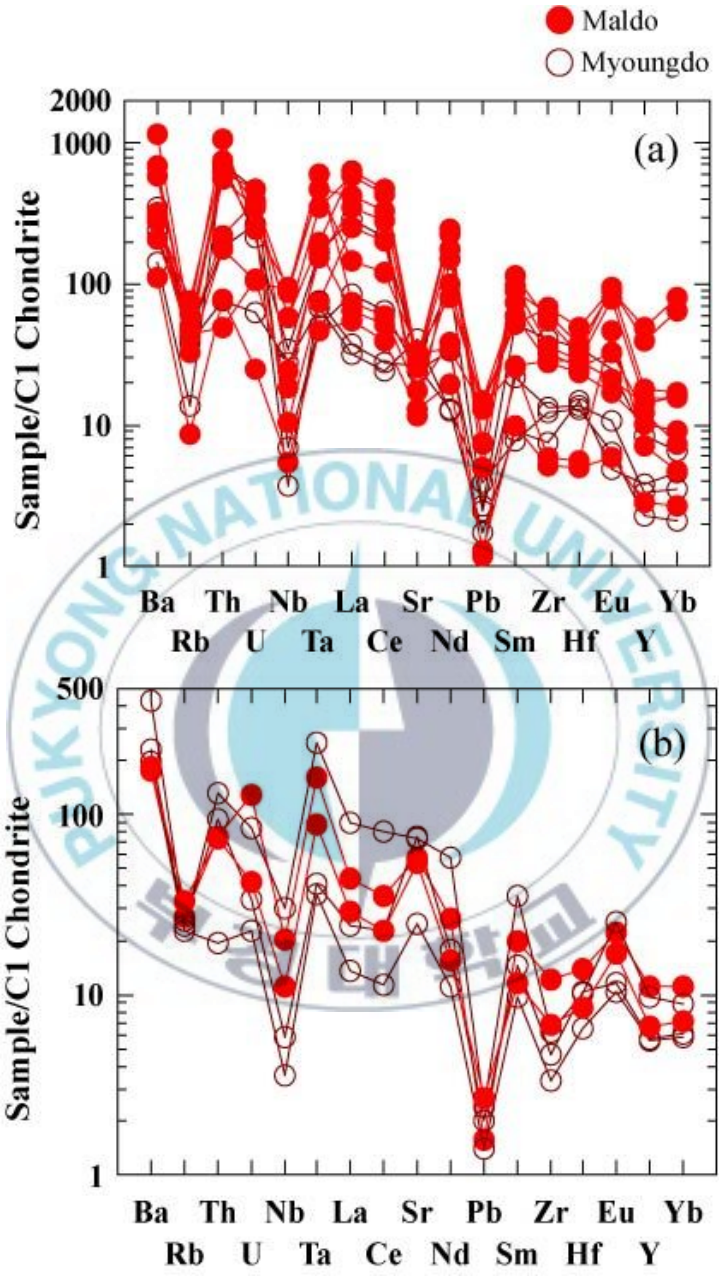

Fig. 27. Chondrite-normalized REE patterns of the meta-granites (a) and metabasites (b) from the study area.

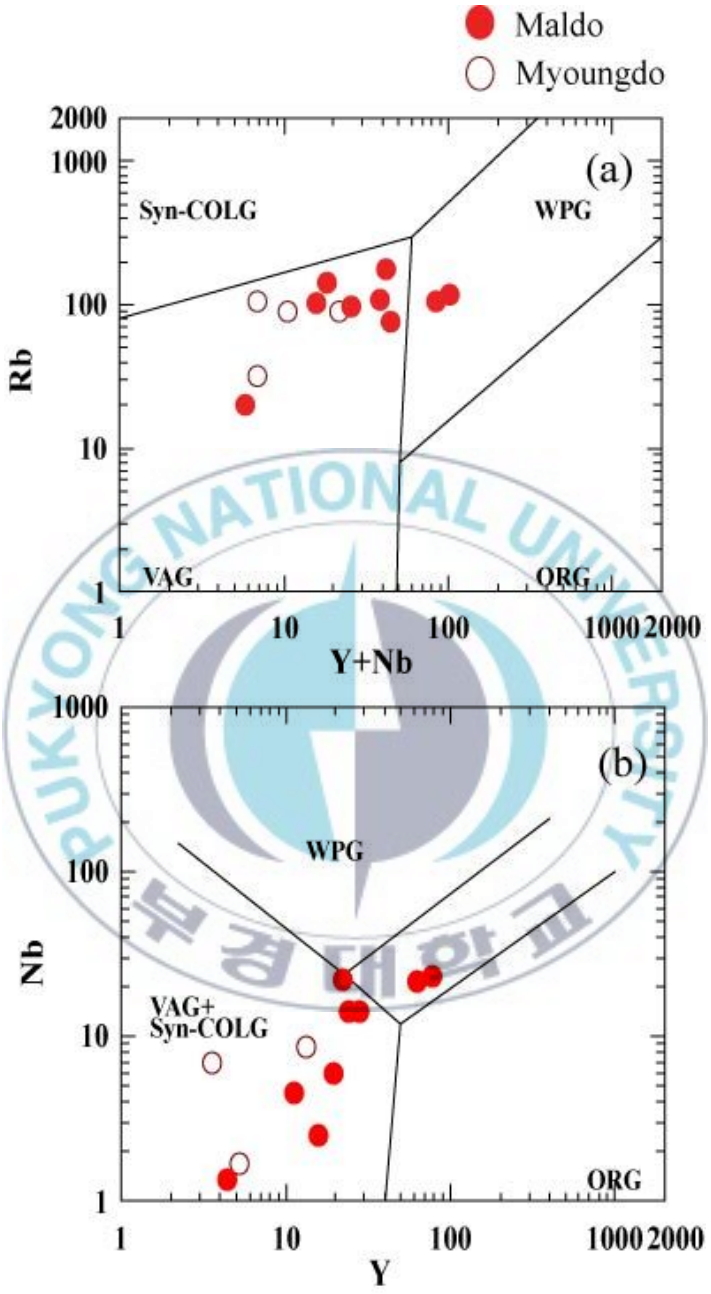

Fig. 28. Tectonic discrimination diagrams for meta-granites from the study area.

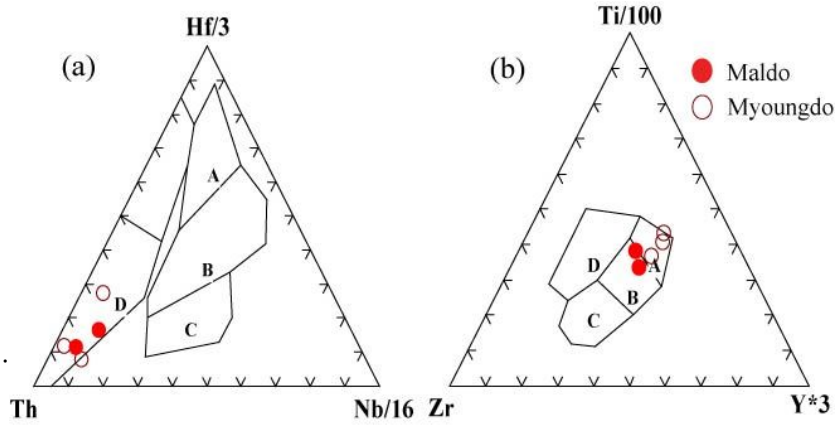

Fig. 29. The Hf-Th-Nb and the Ti-Zr-Y discrimination diagrams (Wood, 1980) for the metabasites in the study area. (a) A, N-type MORB; B, E-type MORB and within-plate basalts and differentiates; C, alkaline within-plate basalts and within-plate basalts and differentiates; D, destructive plate-margin basalts and differentiates. (b) A, IAB; B, MORB & IAB; C, IAB; D, OIB.

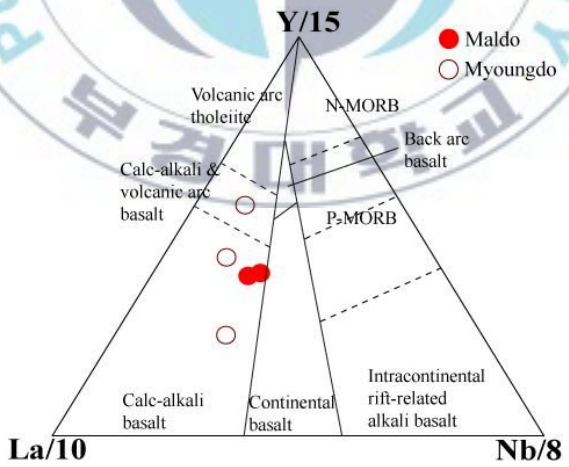

Fig. 30. Y/15-La/10-Nb/8 ternary diagram (after Cabanis and Lecolle, 1989) for the metabasites in the study area.

6. Mineral chemistry

Samples were cut to fit onto a slide-glass using a diamond saw and were pasted whit epoxy resin and dried for 1 day. The surface of cut samples was ground up to 2m on sandpapers in wet condition. Thin sections are then fully polished with a sequence of 6m, 3m and 1m diamond paste steps for electron microprobe analysis.

The polished thin sections were coated with carbon under vacuum in preparation for quantitative, qualitative analysis.

Major element compositions of minerals were analyzed by electron microprobe analysis at the Central Laboratory of Pusan National University, Pukyong National University and Gyeongsang National University using a wavelength dispersive spectrometers.

The analytical condition of Pusan National University EPMA (Cameca SX 100) was 15keV in acceleration voltage, 20nA in beam current and 3~5μm in beam diameter. The analytical condition of Pusan National University EPMA (JXA-8100, JEOL) was 15keV in acceleration voltage, 20nA in beam current and 3~5μm in beam diameter. The analytical condition of Pukyong National University EPMA (SHIMADZU.. EPMA-1600) is same Pusan National University. The analysis used standard materials which conducts P&H Developments Ltd. in England. Sorts and element contents are that albite (Si 32.1%, Na 8.71%), orthoclase (Al 9.81%, K 12.18%), rutile (Ti 59.95%), specullarite (Fe 69.94%), periclase (Mg 60.3%), rhodonite (Mn 32.85%), wollastonite (Ca 34.12%) and chrom (Cr 68.42%).

6-1. Plagioclase

The result of feldspar analysis by electron probe is listed in Table 8.

In Maldo, most feldspars are plotted in albite and just feldspars of meta-granites are plotted in orthoclase domain. In Myeongdo, it is plotted in albite~andesine, orthoclase~andesine (Fig. 31). The reason that element range is wide is owing to difference of formation of origin material.

6-2. Muscovite

The result of muscovite analysis by electron probe is listed in Table 9. Figure 32 shows Si is in inverse proportion to Al except for Maldo sample having in especial a high Fe content but Mg+Fe and Si is counterexample. In fact, muscovite's contents change is explained tschermakite substitution - $(Mg,Fe^{2})+Si=Al^{IV}+Al^{VI}$.

6-3. Amphibole

The result of amphiboles analysis by electron probe in Table 10.

Data of quantitative analyzed amphiboles were used by Minpet program for formular calculation. Formular calculation were estimated by two methods. The first method calculated the contents of Ca, Na and K cations that is 13 (Table 10). The second method meant the contents of

both Na-K cations and Ca-Na-K cations that the contents were 15, 13, respectively, and then, calculated formular.

Si content range from 6.2 to 7.9 in Maldo and from 6.3 to 6.7 in Myeongdo. By the classification of Leake (1997), it is plotted in Mg-hornblende, actinolite and tschermakite. Maldo's amphiboles is plotted in Mg-hornblende and Myeongdo's is plotted in Mg-hornblende and tschermakite (Fig. 33).

6-4. Pyroxene

The result of pyroxene analysis by electron probe in Table 11. Pyroxenes is clinopyroxenes that CaO content is 12.68%, plotted in augite in the classification of pyroxenes (Fig. 34).

6-5. Epidote

The result of epidotes analysis by electron probe in Table 12. Because epidotes are suffered from regional low-metamorphism, it yields secondary ore and used as an index of metamorphic grade. Epidotes in the study area is yielded with metabasites.

6-6. Chlorite

The result of pyroxenes analysis by electron probe in Table 13.

$Mg/Mg+Fe^{2+}$ ranges from 0.613 to 0.626. Chemical compositions of sample mm-27 is similar to Mg ratio of muscovite (0.648~0.662, Table 9) and is the secondary minerals of muscovite under microscope feature.

6-7. Ore minerals

The result of ore minerals analysis by electron probe in Table 14. The result shows that ore minerals are chalcopyrite ($CuFeS_2$), pyrite (FeS_2) and ilmenite ($FeTiO_3$).

Table 8. Representative analyses of Feldspars from the study area.

Sample	mm-24		mm-27							
Lithology	metasedimentary rocks		metabasites							
SiO_2	62.64	60.98	68.92	70.56	63.64	27.27	67.34	67.75	43.23	61.48
Al_2O_3	19.22	18.98	20.51	20.50	22.92	19.80	20.60	20.48	23.12	20.42
CaO	0.16	0.35	0.76	0.28	4.14	0.12	0.74	0.58	17.36	0.73
Na_2O	10.60	10.45	11.45	11.97	9.24	0.00	10.95	11.23	2.38	11.25
K_2O	0.10	0.14	0.10	0.05	0.08	0.04	0.08	0.26	0.08	0.12
MgO	0.02	0.02	0.01	0.00	0.00	17.65	0.00	0.02	0.00	0.01
FeO	0.14	0.13	0.03	0.06	0.16	22.14	0.07	0.08	7.34	0.06
TiO_2	2.85	18.98	0.01	0.02	0.00	0.04	0.02	0.00	0.06	0.01
Total	95.77	94.69	101.79	103.44	100.18	87.06	99.80	100.40	93.57	94.07
(on the basis of 8O)										
Si	2.88	2.84	2.96	2.98	2.81	1.62	2.95	2.95	2.24	2.88
Al	1.04	1.04	1.04	1.02	1.19	1.39	1.06	1.05	1.41	1.13
Ca	0.01	0.02	0.04	0.01	0.20	0.01	0.04	0.03	0.96	0.04
Na	0.94	0.94	0.95	0.98	0.79	0.00	0.93	0.95	0.24	1.02
K	0.01	0.01	0.01	0.00	0.01	0.00	0.00	0.01	0.01	0.01
Fe	0.01	0.00	0.00	0.00	0.01	1.10	0.00	0.00	0.32	0.00
Mg	0.00	0.00	0.00	0.00	0.00	1.56	0.00	0.00	0.00	0.00
Ti	0.00	0.13	0.00	0.00	0.00	0.00	0.00	0.00	0.00	0.00
Total	4.88	4.99	5.00	5.00	5.00	5.69	4.99	5.00	5.18	5.07
An	0.008	0.018	0.035	0.013	0.198	0.700	0.036	0.027	0.798	0.034
Ab	0.986	0.973	0.959	0.984	0.797	0.00	0.960	0.959	0.198	0.959
Or	0.006	0.008	0.006	0.003	0.005	0.300	0.004	0.014	0.004	0.007

* An=Ca/(Ca+Na+K), Ab=Na/(Ca+Na+K), Or=K/(Ca+Na+K)

Table 8. (continued)

Sample	mm-5-1					mm-6b					
Lithology	meta-granites					metasedimentary rocks					
SiO_2	65.76	63.12	98.21	64.24	62.84	64.35	63.97	63.86	62.35	63.24	64.44
Al_2O_3	18.82	17.91	0.05	18.40	17.82	18.80	18.99	19.70	21.89	19.03	18.93
CaO	0.00	0.00	0.02	0.00	0.00	0.15	0.17	0.63	0.05	0.15	0.06
Na_2O	0.29	0.36	0.00	0.46	0.36	11.00	10.92	10.64	10.06	10.40	10.79
K_2O	16.00	15.57	0.03	15.12	15.69	0.05	0.06	0.52	1.23	0.56	0.10
MgO	0.00	0.00	0.00	0.00	0.00	0.00	0.00	0.02	0.04	0.06	0.00
FeO	0.05	0.04	0.03	0.02	0.00	0.21	0.16	0.12	0.10	0.17	0.10
TiO_2	0.00	0.03	0.00	0.02	0.00	0.00	0.03	0.00	0.02	0.04	0.01
Total	100.92	97.03	98.34	98.26	96.71	94.55	94.30	95.49	95.73	93.64	94.42
(on the basis of 8O)											
Si	3.00	3.00	4.00	3.00	3.00	2.98	2.97	2.94	2.86	2.96	2.98
Al	1.01	1.00	0.001	1.01	1.00	1.02	1.04	1.07	1.18	1.05	1.03
Ca	0.00	0.00	0.00	0.001	0.00	0.01	0.01	0.03	0.00	0.01	0.00
Na	0.03	0.03	0.001	0.04	0.03	0.99	0.98	0.95	0.90	0.94	0.97
K	0.93	0.94	0.001	0.90	0.96	0.00	0.00	0.03	0.07	0.03	0.01
Fe	0.00	0.00	0.00	0.001	0.00	0.01	0.01	0.00	0.00	0.01	0.00
Mg	0.00	0.00	0.00	0.001	0.00	0.00	0.00	0.00	0.00	0.00	0.00
Ti	0.00	0.00	0.003	0.003	0.00	0.00	0.00	0.00	0.00	0.00	0.00
Total	4.97	4.98	4.00	4.96	4.99	5.01	5.01	5.02	5.03	5.00	4.99
An	0.000	0.000	0.500	0.000	0.000	0.007	0.008	0.031	0.002	0.007	0.003
Ab	0.026	0.034	0.000	0.044	0.034	0.990	0.988	0.939	0.923	0.959	0.991
Or	0.974	0.966	0.500	0.956	0.966	0.003	0.004	0.030	0.074	0.034	0.006

* An=Ca/(Ca+Na+K), Ab=Na/(Ca+Na+K), Or=K/(Ca+Na+K)

Table 8. (continued)

Sample	mm-6c						mm-9a			
Lithology	meta-granites						metabasites			
SiO_2	65.88	62.75	66.54	67.58	67.82	66.12	69.97	66.78	66.03	68.27
Al_2O_3	19.71	20.5	19.65	20.26	20.48	20.31	20.55	20.53	21.2	20.34
CaO	0.75	0.35	0.78	1.18	0.95	0.23	0.57	1.32	0.67	0.66
Na_2O	10.56	9.07	10.97	11.09	11.26	10.47	11.59	10.83	10.55	11.39
K_2O	0.11	1.9	0.12	0.12	0.3	0.75	0.07	0.1	0.94	0.09
MgO	0.00	0.3	0.03	0.00	0.00	0.07	0.01	0.00	0.12	0.01
FeO	0.00	0.62	0.04	0.04	0.07	0.23	0.09	0.05	0.21	0.11
TiO_2	0.01	0.00	0.01	0.00	0.00	0.00	0.01	0.01	0.01	0.03
Total	97.02	95.49	98.14	100.27	100.88	98.18	102.86	99.62	99.73	100.90
(on the basis of 8O)										
Si	2.965	2.9	2.966	2.953	2.948	2.95	2.973	2.937	2.911	2.961
Al	1.046	1.117	1.033	1.043	1.049	1.068	1.029	1.064	1.101	1.04
Ca	0.036	0.017	0.037	0.055	0.044	0.011	0.026	0.062	0.032	0.031
Na	0.922	0.812	0.949	0.939	0.949	0.906	0.955	0.924	0.902	0.958
K	0.007	0.112	0.007	0.007	0.016	0.043	0.004	0.005	0.053	0.005
Fe	0.000	0.024	0.002	0.001	0.003	0.009	0.003	0.002	0.008	0.004
Mg	0.000	0.021	0.002	0.000	0.000	0.004	0.001	0.000	0.008	0.000
Ti	0.000	0.000	0.000	0.000	0.000	0.000	0.000	0.000	0.000	0.001
Total	4.98	5.00	5.00	5.00	5.01	4.99	4.99	4.99	5.02	5.00
An	0.037	0.018	0.037	0.055	0.044	0.011	0.026	0.063	0.032	0.031
Ab	0.955	0.863	0.956	0.938	0.941	0.944	0.970	0.932	0.914	0.964
Or	0.007	0.119	0.007	0.007	0.016	0.045	0.004	0.005	0.054	0.005

* An=Ca/(Ca+Na+K), Ab=Na/(Ca+Na+K), Or=K/(Ca+Na+K)

Table 8. (continued)

Sample	mm-9b			mm-10					
Lithology	metabasites			metabasites					
SiO_2	67.40	65.24	67.69	68.05	68.92	56.71	67.78	69.61	68.34
Al_2O_3	19.91	21.47	20.07	19.79	19.74	17.58	19.96	20.22	19.92
CaO	0.65	0.53	0.60	0.33	0.26	5.14	0.39	0.21	0.23
Na_2O	11.39	10.13	11.36	11.41	11.64	9.54	11.26	11.65	11.59
K_2O	0.06	1.18	0.06	0.12	0.04	0.36	0.07	0.09	0.05
MgO	0.01	0.22	0.02	0.03	0.02	2.43	0.02	0.01	0.01
FeO	0.04	0.21	0.00	0.00	0.03	2.00	0.08	0.02	0.00
TiO_2	0.00	0.01	0.00	0.00	0.00	0.03	0.02	0.00	0.01
Total	99.46	98.99	99.80	99.73	100.65	93.79	99.58	101.81	100.15
(on the basis of 8O)									
Si	2.965	2.898	2.966	2.981	2.99	2.752	2.973	2.985	2.98
Al	1.032	1.124	1.036	1.022	1.01	1.006	1.032	1.022	1.024
Ca	0.031	0.025	0.028	0.016	0.012	0.267	0.019	0.01	0.011
Na	0.972	0.872	0.965	0.969	0.979	0.898	0.958	0.968	0.98
K	0.003	0.067	0.004	0.007	0.002	0.023	0.004	0.005	0.003
Fe	0.002	0.008	0.000	0.000	0.001	0.081	0.003	0.001	0.000
Mg	0.001	0.014	0.001	0.002	0.001	0.176	0.001	0.001	0.001
Ti	0.000	0.000	0.000	0.000	0.000	0.001	0.001	0.000	0.000
Total	5.006	5.008	5.000	5.00	5.00	5.20	4.99	4.99	5.00
An	0.031	0.026	0.028	0.016	0.012	0.225	0.019	0.010	0.011
Ab	0.966	0.905	0.968	0.977	0.986	0.756	0.977	0.985	0.986
Or	0.003	0.070	0.004	0.007	0.002	0.019	0.004	0.005	0.003

* An=Ca/(Ca+Na+K), Ab=Na/(Ca+Na+K), Or=K/(Ca+Na+K)

Table 8. (continued)

Sample	mm-10					mm-24	
Lithology	metabasites					metasedimentary rocks	
SiO_2	68.95	67.78	67.49	65.36	67.45	62.64	60.98
Al_2O_3	20.03	20.00	20.99	19.42	19.07	19.22	18.98
CaO	0.44	0.71	0.69	0.32	0.31	0.16	0.35
Na_2O	11.53	11.24	10.80	11.16	10.95	10.60	10.45
K_2O	0.07	0.09	0.72	0.06	0.07	0.10	0.14
MgO	0.00	0.01	0.17	0.01	0.01	0.02	0.02
FeO	0.00	0.00	0.27	0.01	0.09	0.14	0.13
TiO_2	0.00	0.00	0.00	0.01	0.01	2.85	18.98
Total	101.02	99.83	101.13	96.34	97.95	95.77	94.69
(on the basis of 8O)							
Si	2.982	2.969	2.931	2.966	3.003	2.876	2.841
Al	1.021	1.033	1.074	1.039	1.000	1.040	1.042
Ca	0.021	0.033	0.032	0.015	0.015	0.008	0.018
Na	0.966	0.954	0.910	0.982	0.945	0.944	0.943
K	0.004	0.005	0.040	0.004	0.004	0.006	0.008
Fe	0.000	0.000	0.010	0.000	0.003	0.005	0.005
Mg	0.000	0.000	0.011	0.001	0.000	0.002	0.001
Ti	0.000	0.000	0.000	0.000	0.000	0.002	0.128
Total	4.994	4.994	5.008	5.007	4.972	4.882	4.986
An	0.021	0.033	0.033	0.015	0.015	0.008	0.018
Ab	0.975	0.962	0.927	0.981	0.980	0.986	0.973
Or	0.004	0.005	0.041	0.004	0.004	0.006	0.008

* An=Ca/(Ca+Na+K), Ab=Na/(Ca+Na+K), Or=K/(Ca+Na+K)

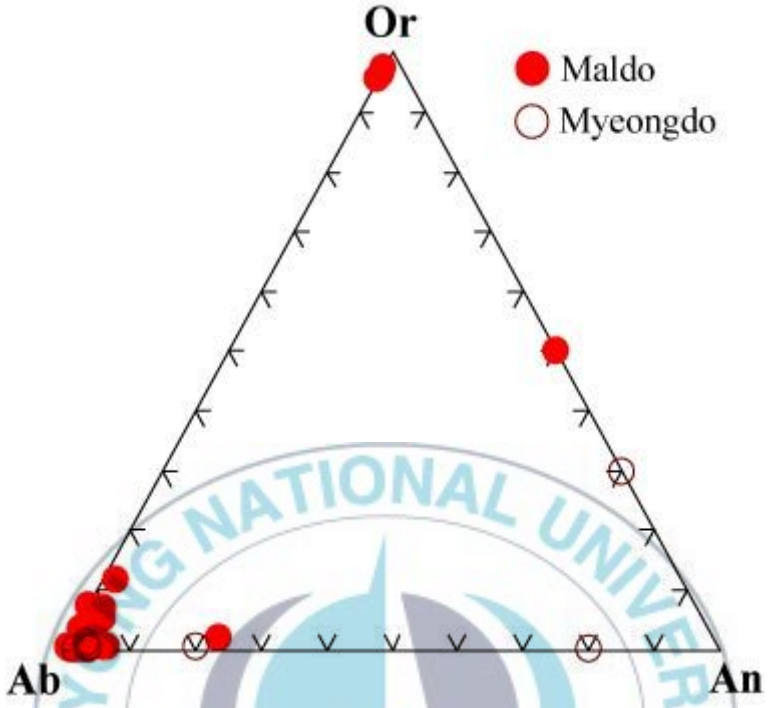

Fig 31. An-Ab-Or ternary diagram for the compositions of feldspars from the study area.

Table 9. Representative analyses of Muscovites from the study area.

Sample	mm-4a				mm-5-1		mm-6c		
Lithology	metasedimentary rocks				meta-granites		meta-granites		
SiO_2	43.51	44.01	44.38	45.73	43.44	45.42	41.13	45.65	44.5
TiO_2	0.16	0.18	0.17	0.06	0.42	1.85	1.6	0.34	0.08
Al_2O_3	30.84	30.42	31.21	32.42	27.29	33.48	22.79	29.2	35.83
FeO	2.79	2.97	3.1	2.65	3.38	1.52	3.06	3.31	0.44
MnO	0.00	0.00	0.00	0.01	0.03	0.02	0.03	0.04	0.00
MgO	0.77	0.81	0.83	0.82	0.56	0.57	1.24	1.66	0.28
CaO	0.00	0.00	0.00	0.00	0.02	0.00	0.14	0.06	0.06
Na_2O	0.56	0.66	0.61	0.56	0.03	0.34	0.09	0.15	0.19
K_2O	9.55	9.3	9.48	10.02	9.22	10.3	8	10.92	8.77
Total	88.18	88.35	89.78	92.27	84.39	93.5	78.08	91.33	90.15
(on the basis of 22O)									
Si	6.303	6.362	6.313	6.32	6.574	6.174	6.746	6.442	6.165
Al^{IV}	1.697	1.638	1.687	1.68	1.426	1.826	1.254	1.558	1.835
Al^{VI}	3.567	3.546	3.545	3.602	3.442	3.537	3.151	3.299	4.015
Ti	0.017	0.019	0.018	0.007	0.047	0.189	0.197	0.036	0.008
Fe	0.338	0.359	0.369	0.306	0.427	0.173	0.42	0.39	0.051
Mn	0.00	0.00	0.00	0.001	0.004	0.003	0.004	0.005	0.00
Mg	0.166	0.175	0.177	0.169	0.127	0.115	0.303	0.35	0.059
Ca	0.00	0.00	0.00	0.00	0.003	0.00	0.025	0.009	0.009
Na	0.157	0.184	0.169	0.151	0.008	0.088	0.03	0.04	0.052
K	1.765	1.715	1.72	1.766	1.781	1.787	1.675	1.966	1.551
Total	14.01	13.998	13.998	14.002	13.839	13.892	13.805	14.095	13.745
X_{Mg}	0.329	0.328	0.324	0.356	0.229	0.399	0.419	0.473	0.536

* X_{Mg}=Mg/(Mg+Fe)

Table 9. (continued)

Sample	mm-6c		mm-9a		mm-9b			
Lithology	meta-granites		metabasites		metabasites			
SiO_2	46.51	46.85	47.53	48.38	46.67	47.08	45.321	45.51
TiO_2	4.63	0.11	0.58	0.65	0.97	1.08	0.978	0.898
Al_2O_3	25.68	26.46	9.28	8.72	8.95	8.93	8.85	8.335
FeO	3.96	3.64	15.03	15	14.67	14.49	13.803	13.77
MnO	0.02	0.05	0.34	0.35	0.33	0.27	0.3	0.335
MgO	2.27	2.24	12.93	13.04	12.69	12.56	12.44	12.654
CaO	0.00	0.00	11.46	11.45	11.27	11.11	11.378	11.149
Na_2O	0.08	0.11	1.13	1.12	1.16	1.1	1.101	1.013
K_2O	10.52	10.78	0.34	0.33	0.45	0.39	0.461	0.486
Total	93.67	90.24	98.62	99.04	97.16	97.01	94.632	94.15
(on the basis of 22O)								
Si	6.507	6.787	6.616	5.330	6.612	6.680	6.575	6.630
Al^{IV}	1.493	1.213	1.384	0.755	1.388	1.320	1.425	1.370
Al^{VI}	1.330	1.799	0.138	0.000	0.107	0.174	0.088	0.062
Ti	0.487	0.012	0.061	0.054	0.103	0.116	0.107	0.098
Fe	0.583	0.882	1.750	2.764	1.738	1.719	1.675	1.678
Mn	0.005	0.012	0.040	0.065	0.040	0.033	0.037	0.041
Mg	0.947	0.967	2.683	4.283	2.679	2.656	2.690	2.748
Ca	0.000	0.000	1.709	2.703	1.710	1.690	1.769	1.740
Na	0.022	0.031	0.304	0.239	0.320	0.302	0.310	0.286
K	1.878	1.992	0.060	0.046	0.081	0.071	0.085	0.090
Total	13.251	13.695	14.745	16.239	14.778	14.761	14.759	14.744
X_{Mg}	0.619	0.523	0.605	0.608	0.607	0.607	0.616	0.621

* X_{Mg}=Mg/(Mg+Fe)

Table 9. (continued)

Sample	mm-24		mm-27a	
Lithology	metasedimentary rocks		metabasites	
SiO_2	44.79	43.81	44	48.89
TiO_2	0.59	0.34	0.06	0.07
Al_2O_3	32.77	33.21	26.05	24.51
FeO	3.15	3.08	5.63	3.94
MnO	0	0	0.03	0.03
MgO	1.25	1.14	6.2	4.08
CaO	0.01	0	0.04	0.01
Na_2O	0.46	0.44	0.07	0.07
K_2O	6.51	6.66	4.6	6.21
Total	89.52	88.67	86.67	87.8
(on the basis of 22O)				
Si	6.257	6.187	6.404	6.954
Al^{IV}	1.743	1.813	1.596	1.046
Al^{VI}	3.652	3.713	2.873	3.064
Ti	0.062	0.036	0.006	0.008
Fe	0.368	0.363	0.685	0.469
Mn	0	0	0.004	0.003
Mg	0.259	0.241	1.344	0.865
Ca	0.001	0	0.007	0.001
Na	0.124	0.121	0.02	0.019
K	1.16	1.199	0.853	1.127
Total	13.626	13.673	13.792	13.556
X_{Mg}	0.413	0.399	0.662	0.648

* X_{Mg}=Mg/(Mg+Fe)

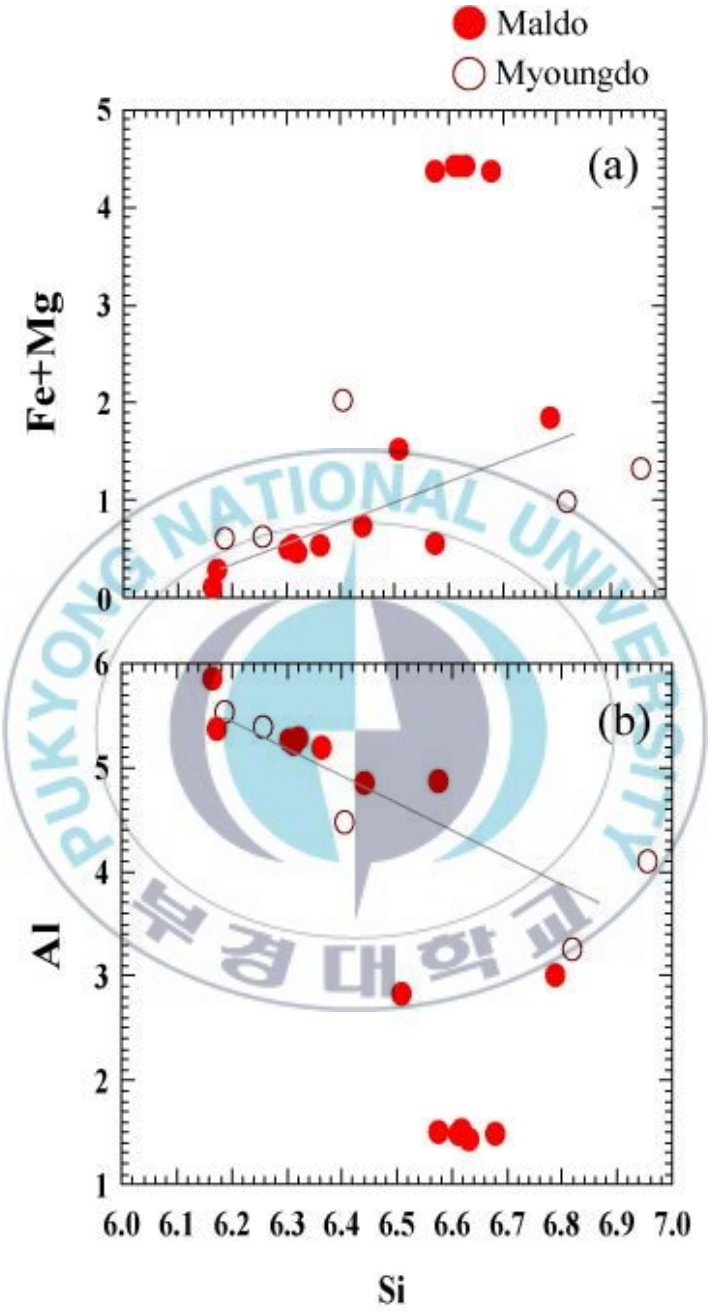

Fig. 32. Fe+Mg vs. Si and Al vs. Si diagrams for the compositions of muscovites from the study area.

Table 10. Representative analyses of Amphiboles from the study area.

Sample	mm-9a					
Lithology	metabasites					
SiO_2	52.98	46.78	49.08	48.72	49.26	51.34
Al_2O_3	3.30	7.61	7.69	8.19	6.20	5.54
TiO_2	0.24	0.63	0.59	0.62	0.55	0.50
Cr_2O_3	0.02	0.09	0.00	0.00	0.00	0.00
FeO	14.01	14.60	14.29	14.75	14.30	14.19
MgO	14.60	12.87	13.27	13.41	13.99	14.66
MnO	0.39	0.32	0.39	0.39	0.40	0.34
CaO	12.21	11.25	11.27	11.02	11.18	11.68
Na_2O	0.63	1.21	1.12	1.03	0.79	0.79
K_2O	0.13	0.39	0.33	0.35	0.24	0.20
Total	98.51	95.75	98.03	98.48	96.91	99.24
	(on the basis of 23O)					
Si	7.61	6.97	7.10	7.00	7.17	7.29
Al^{IV}	0.39	1.04	0.90	1.00	0.83	0.71
Al^{VI}	0.17	0.30	0.41	0.38	0.23	0.22
Mg	3.13	2.86	2.86	2.87	3.04	3.10
Fe^{2+}	1.51	1.36	1.31	1.18	1.17	1.24
Ti	0.03	0.07	0.06	0.07	0.06	0.05
Fe^{2+}	0.03	0.08	0.09	0.12	0.10	0.08
Mn	0.02	0.02	0.02	0.02	0.03	0.02
Ca	1.88	1.80	1.75	1.70	1.74	1.78
Na	0.06	0.11	0.13	0.14	0.11	0.11
Ca	0.00	0.00	0.00	0.00	0.00	0.00
Na	0.11	0.24	0.18	0.15	0.11	0.11
K	0.02	0.07	0.06	0.06	0.05	0.04
Total	14.96	14.91	14.89	14.69	14.63	14.75
X_{Mg}	0.67	0.68	0.69	0.71	0.72	0.71

* X_{Mg}=Mg/(Mg+Fe)

Table 10. (continued)

Sample	mm-9b									
Lithology	metabasites									
SiO_2	49.54	49.59	51.82	51.34	48.09	44.80	46.47	49.00	50.35	43.75
Al_2O_3	6.58	4.65	4.77	4.33	8.07	8.88	8.39	5.55	4.43	7.31
TiO_2	0.71	0.43	0.54	0.48	0.90	1.32	0.91	0.61	0.51	0.42
Cr_2O_3	0.00	0.00	0.00	0.00	0.00	0.00	0.00	0.00	0.00	0.00
FeO	13.74	12.07	13.64	13.09	14.67	13.91	13.46	12.77	12.00	15.56
MgO	14.23	14.73	15.46	15.48	13.03	12.14	12.49	14.37	14.80	15.25
MnO	0.32	0.32	0.24	0.31	0.30	0.30	0.33	0.29	0.26	0.25
CaO	11.34	11.68	11.60	11.73	11.42	11.42	11.56	11.56	11.99	8.21
Na_2O	0.90	0.68	0.56	0.58	1.02	0.99	1.01	0.62	0.46	0.89
K_2O	0.30	0.19	0.21	0.18	0.35	0.43	0.45	0.25	0.23	0.21
Total	97.66	94.33	98.84	97.52	97.85	94.18	95.07	95.03	95.01	91.82
(on the basis of 23O)										
Si	7.16	7.39	7.35	7.38	6.99	6.79	6.97	7.25	7.44	6.58
Al^{IV}	0.84	0.61	0.66	0.62	1.02	1.21	1.04	0.75	0.56	1.26
Al^{VI}	0.28	0.20	0.14	0.11	0.37	0.37	0.45	0.22	0.21	0.03
Mg	3.06	3.27	3.27	3.32	2.82	2.74	2.79	3.17	3.26	3.42
Fe^{2+}	1.18	1.23	1.06	1.08	1.35	1.40	1.44	1.18	1.29	0.30
Ti	0.08	0.05	0.06	0.05	0.10	0.15	0.10	0.07	0.06	0.05
Fe^{2+}	0.10	0.04	0.10	0.07	0.09	0.05	0.05	0.06	0.03	0.31
Mn	0.02	0.02	0.02	0.02	0.02	0.02	0.02	0.02	0.02	0.02
Ca	1.76	1.86	1.76	1.81	1.78	1.85	1.86	1.83	1.90	1.32
Na	0.13	0.07	0.08	0.08	0.12	0.08	0.08	0.09	0.05	0.13
Ca	0.00	0.00	0.00	0.00	0.00	0.00	0.00	0.00	0.00	0.00
Na	0.13	0.12	0.08	0.08	0.17	0.21	0.22	0.09	0.08	0.13
K	0.06	0.04	0.04	0.03	0.07	0.08	0.09	0.05	0.04	0.04
Total	14.77	14.91	14.59	14.65	14.87	14.96	15.09	14.78	14.94	13.57
X_{Mg}	0.72	0.73	0.76	0.75	0.68	0.66	0.66	0.73	0.72	0.92

* X_{Mg}=Mg/(Mg+Fe)

Table 10. (continued)

Sample	mm-10					
Lithology	metabasites					
SiO_2	48.29	46.75	49.88	46.29	44.42	41.20
Al_2O_3	5.27	8.53	4.70	8.61	10.32	11.35
TiO_2	0.16	0.54	0.37	1.35	1.31	0.17
Cr_2O_3	0.00	0.00	0.00	0.00	0.05	0.00
FeO	16.22	16.25	15.69	15.69	16.12	17.17
MgO	14.60	12.61	13.78	11.44	11.27	13.95
MnO	0.34	0.32	0.30	0.30	0.32	0.38
CaO	10.16	10.59	11.65	11.51	11.64	7.74
Na_2O	0.28	1.06	0.34	1.18	1.16	0.49
K_2O	0.17	0.59	0.25	0.62	0.83	0.48
Total	95.49	97.24	96.96	96.99	97.44	92.94
	(on the basis of 23O)					
Si	7.06	6.85	7.28	6.89	6.59	6.11
Al^{IV}	0.87	1.15	0.72	1.11	1.41	1.83
Al^{VI}	0.04	0.32	0.09	0.40	0.39	0.16
Mg	3.18	2.75	3.00	2.54	2.49	3.08
Fe^{2+}	0.55	1.19	1.26	1.70	1.55	0.18
Ti	0.02	0.06	0.04	0.15	0.15	0.02
Fe^{2+}	0.17	0.14	0.06	0.06	0.05	0.34
Mn	0.02	0.02	0.02	0.02	0.02	0.03
Ca	1.59	1.66	1.82	1.84	1.85	1.23
Na	0.04	0.15	0.05	0.09	0.08	0.07
Ca	0.00	0.00	0.00	0.00	0.00	0.00
Na	0.04	0.15	0.05	0.25	0.25	0.07
K	0.03	0.11	0.05	0.12	0.16	0.09
Total	13.62	14.55	14.44	15.15	14.99	13.21
X_{Mg}	0.85	0.70	0.70	0.60	0.62	0.94

* X_{Mg}=Mg/(Mg+Fe)

Table 10. (continued)

Sample	mm-27										
Lithology	metabasites										
SiO_2	44.90	40.81	41.35	45.04	42.24	42.99	42.11	42.31	42.84	41.73	41.08
Al_2O_3	10.20	10.17	10.26	10.23	9.27	9.15	10.26	10.13	9.83	9.32	10.11
TiO_2	1.19	1.19	1.16	1.39	0.97	1.14	1.17	1.21	1.11	1.00	1.15
Cr_2O_3	0.00	0.00	0.00	0.00	0.00	0.00	0.00	0.00	0.00	0.00	0.00
FeO	16.27	15.42	15.87	16.01	14.33	14.22	14.86	14.63	14.48	14.87	15.61
MgO	11.52	11.23	11.24	11.26	12.37	12.02	11.66	11.99	11.86	11.27	10.96
MnO	0.36	0.28	0.32	0.32	0.36	0.32	0.32	0.32	0.28	0.30	0.27
CaO	11.68	11.68	11.39	11.77	11.72	11.80	11.53	11.52	11.79	11.38	11.48
Na_2O	1.25	1.27	1.29	1.16	1.16	1.11	1.32	1.15	1.18	1.17	1.25
K_2O	0.92	1.09	1.12	0.74	0.88	0.91	0.99	1.00	0.99	1.03	1.10
Total	98.29	93.14	94.00	97.92	93.30	93.64	94.22	94.27	94.37	92.07	93.01
	(on the basis of 23O)										
Si	6.60	6.36	6.38	6.64	6.51	6.61	6.45	6.46	6.55	6.56	6.42
Al^{IV}	1.40	1.64	1.62	1.36	1.50	1.39	1.55	1.54	1.45	1.44	1.58
Al^{VI}	0.37	0.23	0.24	0.42	0.19	0.27	0.31	0.28	0.32	0.29	0.28
Mg	2.53	2.61	2.59	2.48	2.84	2.76	2.66	2.73	2.70	2.64	2.55
Fe^{2+}	1.55	1.42	1.39	1.62	1.20	1.42	1.38	1.26	1.42	1.49	1.50
Ti	0.13	0.14	0.13	0.15	0.11	0.13	0.14	0.14	0.13	0.12	0.14
Fe^{2+}	0.05	0.01	0.03	0.05	0.01	0.01	0.03	0.03	0.01	0.02	0.02
Mn	0.02	0.02	0.02	0.02	0.02	0.02	0.02	0.02	0.02	0.02	0.02
Ca	1.84	1.95	0.00	1.86	1.93	1.94	1.89	1.88	1.93	1.92	1.92
Na	0.09	0.03	0.06	0.08	0.04	0.03	0.06	0.06	0.04	0.05	0.04
Ca	0.00	0.00	0.00	0.00	0.00	0.00	0.00	0.00	0.00	0.00	0.00
Na	0.27	0.36	0.32	0.26	0.31	0.30	0.34	0.28	0.31	0.31	0.34
K	0.00	0.22	0.22	0.14	0.17	0.18	0.19	0.20	0.19	0.21	0.22
Total	14.85	14.97	13.01	15.07	14.82	15.05	15.01	14.88	15.07	15.05	15.01
X_{Mg}	0.62	0.65	0.65	0.60	0.70	0.66	0.66	0.68	0.65	0.64	0.63

* X_{Mg}=Mg/(Mg+Fe)

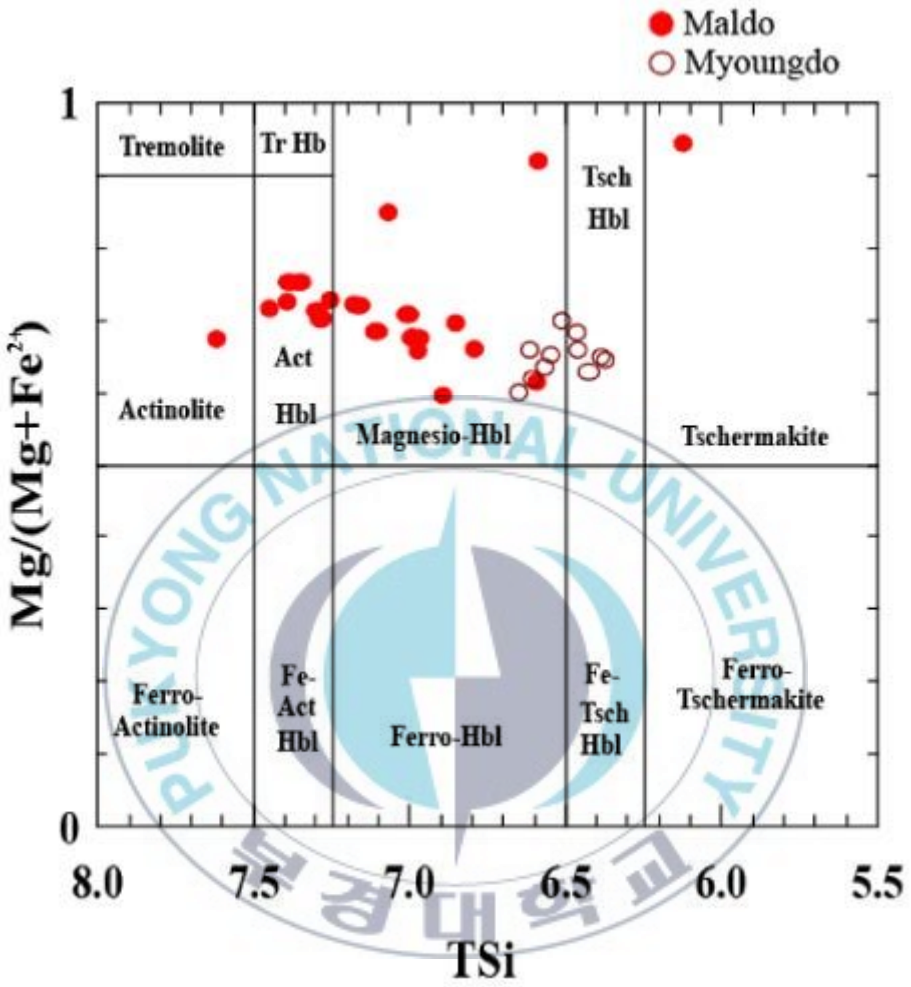

Fig. 33. Mg/(Mg+Fe2+) vs. TSi diagram for the compositions of amphiboles from the study area, (after Leake et al., 1997)

Table 11. Representative analyses of Clinopyroxenes from the study area.

Sample	mm-10		mm-9b
Lithology	metabasites		metabasites
SiO_2	54.91	55.01	55.18
Al_2O_3	0.72	0.47	0.72
TiO_2	0.00	0.00	0.04
Cr_2O_3	0.05	0.00	0.00
FeO	12.70	9.72	17.46
MgO	16.71	17.81	13.81
MnO	0.15	0.26	0.30
CaO	12.68	12.60	12.68
Na_2O	0.02	0.13	0.12
K_2O	0.04	0.01	0.03
Total	97.98	96.01	100.34
(on the basis of 6O)			
Si	2.05	2.07	2.06
Al	0.00	0.00	0.00
Al	0.03	0.02	0.03
Fe^{2+}	0.40	0.31	0.54
Ti^{4+}	0.00	0.00	0.00
Mg	0.93	1.00	0.77
Mn	0.00	0.01	0.01
Ca	0.51	0.51	0.51
Na	0.00	0.01	0.01
k	0.00	0.00	0.00
Total	3.93	3.92	3.93
Xmg	0.507	0.551	0.422
Xca	0.277	0.280	0.279
Xfe	0.216	0.169	0.299

* Xmg=Mg/(Mg+Fe), Xca=Ca/(Mg+Fe), Xfe=Fe/(Mg+Fe)

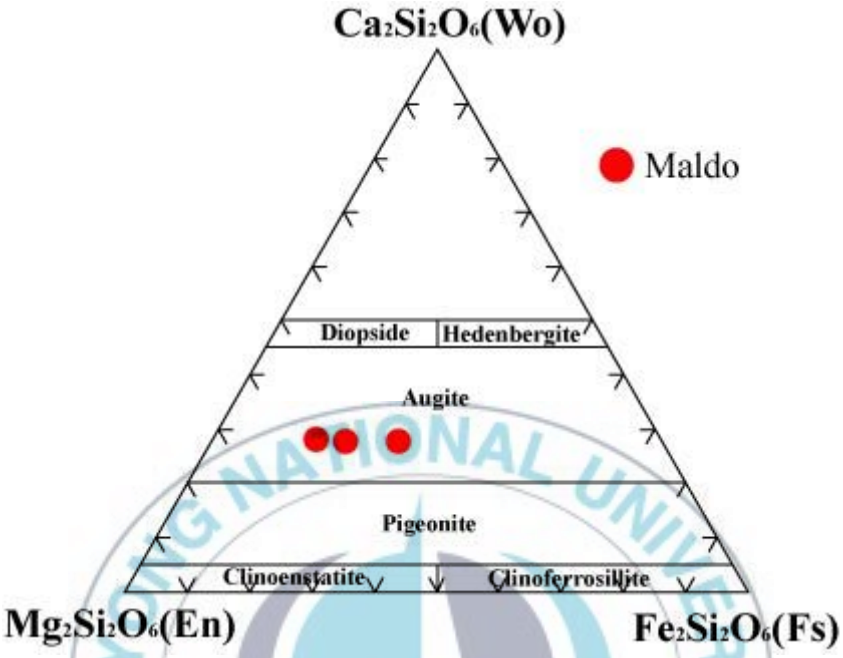

Fig. 34. Wo-En-Fs ternary diagram for the compositions of clinopyroxenes from the study area.

Table 12. Representative analyses of Epidotes from the study area.

Sample	mm-9b					
Lithology	metabasites					
SiO_2	38.35	35.84	38.66	38.41	38.61	37.95
TiO_2	0.05	0.14	0.09	0.05	0.13	0.02
Al_2O_3	27.30	9.18	28.26	28.89	28.73	28.23
FeO	6.17	15.93	4.96	4.60	4.52	5.19
MnO	0.10	0.46	0.06	0.10	0.31	0.12
MgO	0.02	13.50	0.02	0.04	0.37	0.05
CaO	23.45	12.92	23.55	23.75	22.75	23.55
Na_2O	0.01	0.18	0.03	0.01	0.01	0.00
K_2O	0.03	0.11	0.00	0.01	0.00	0.01
Total	95.48	88.27	95.63	95.85	95.42	95.12
(on the basis of 12.5O)						
Si	5.920	6.322	5.914	5.856	5.895	5.854
Ti	0.006	0.019	0.011	0.006	0.015	0.002
Al	4.968	1.910	5.095	5.191	5.171	5.132
Fe	0.797	2.351	0.634	0.586	0.577	0.670
Mg	0.004	3.550	0.004	0.010	0.083	0.011
Mn	0.013	0.069	0.008	0.013	0.040	0.015
Ca	3.880	2.442	3.859	3.880	3.722	3.892
Na	0.003	0.061	0.008	0.002	0.003	0.000
K	0.006	0.025	0.000	0.001	0.000	0.002
Total	15.595	16.748	15.532	15.544	15.507	15.578

Table 12. (continued)

Sample	mm-10							
Lithology	metabasites							
SiO_2	38.40	37.90	38.92	38.44	38.50	37.96	50.00	38.10
TiO_2	0.06	0.08	0.06	0.03	0.09	0.03	0.31	0.09
Al_2O_3	26.21	27.50	26.59	27.31	27.01	26.78	5.83	26.62
FeO	7.12	5.56	6.74	6.32	6.78	6.97	13.53	7.02
MnO	0.04	0.09	0.07	0.08	0.07	0.05	0.33	0.12
MgO	0.02	0.03	0.01	0.02	0.01	0.03	13.50	0.02
CaO	23.90	23.71	23.91	24.02	23.56	23.58	12.21	23.28
Na_2O	0.04	0.00	0.05	0.03	0.03	0.01	0.43	0.02
K_2O	0.01	0.00	0.03	0.02	0.00	0.00	0.16	0.02
Total	95.79	94.88	96.36	96.25	96.03	95.41	96.28	95.30
(on the basis of 12.5O)								
Si	5.950	5.879	5.975	5.900	5.927	5.896	7.688	5.923
Ti	0.007	0.009	0.007	0.004	0.010	0.003	0.036	0.011
Al	4.787	5.029	4.813	4.941	4.901	4.904	1.056	4.878
Fe	0.922	0.722	0.865	0.812	0.873	0.905	1.740	0.913
Mg	0.004	0.006	0.001	0.005	0.001	0.008	3.094	0.004
Mn	0.006	0.012	0.009	0.010	0.009	0.007	0.043	0.015
Ca	3.968	3.941	3.933	3.950	3.886	3.924	2.011	3.878
Na	0.011	0.000	0.014	0.008	0.008	0.004	0.128	0.006
K	0.001	0.000	0.005	0.003	0.001	0.001	0.031	0.004
Total	15.656	15.598	15.622	15.631	15.616	15.651	15.828	15.632

Table 13. Representative analyses of Chlorites from the study area.

Sample	mm-27					
Lithology	metabasites					
SiO_2	28.65	29.56	27.77	26.31	25.25	26.49
Al_2O_3	16.95	17.61	18.13	0.09	0.11	0.80
TiO_2	0.79	0.19	0.15	19.10	19.38	19.09
FeO	20.84	21.53	21.39	19.79	20.27	19.61
MnO	0.28	0.28	0.34	0.36	0.39	0.34
MgO	18.50	19.50	18.97	18.20	19.01	17.63
CaO	0.53	0.07	0.03	0.04	0.02	0.68
Na_2O	0.02	0.00	0.00	0.01	0.00	0.00
K_2O	0.45	0.24	0.19	0.03	0.04	0.19
Total	87.01	88.98	86.97	83.92	84.46	84.81
(on the basis of 20O)						
Si	4.258	4.282	4.132	4.836	4.641	4.825
AI^{IV}	2.969	3.006	3.179	3.164	3.359	3.175
Al^{VI}	0.000	0.000	0.000	0.974	0.840	0.924
Ti	0.088	0.021	0.017	0.012	0.015	0.110
Mg	4.098	4.210	4.207	4.987	5.207	4.789
Fe	2.590	2.608	2.662	3.042	3.115	2.987
Mn	0.035	0.034	0.043	0.057	0.060	0.052
Ca	0.084	0.011	0.005	0.007	0.004	0.132
Na	0.006	0.000	0.000	0.002	0.000	0.000
K	0.085	0.044	0.036	0.007	0.010	0.043
Total	14.215	14.217	14.280	17.088	17.250	17.037
X_{Mg}	0.613	0.617	0.613	0.621	0.626	0.616

* Xmg=Mg/(Mg+Fe)

Table 14. Semi-quantitative analyses of the compositions of opaque minerals from the study area.

Sample	mm-10d				mm-27a
Lithology	metabasites				metabasites
minerals	ilmenite	pyrite	chalcopyrite	pyrite	pyrite
Fe	37.58	45.01	32.94	45.45	46.01
Ti	45.76	0.00	0.00	0.00	0.00
S	0.00	54.10	35.35	54.55	53.01
Cu	0.00	0.00	31.712	0.00	0.00
O	16.66	0.00	0.00	0.00	0.00
Total	100	100	100	100	99.02

7. Metamorphism

Metabasites which are distributed on Maldo and Myeongdo are selected and made thin section. The metamorphic mineral assemblages in the sample mm-9a, b and mm-10 consist of quartz + muscovite + amphibole + epidote. The metamorphic mineral groups in the sample mm-27a are the same as the metamorphic mineral assemblages of Maldo.

To calculate metamorphic temperature and press of the metabasites in the study area, a GeoThermoBarometry (Kohn and Spear, 1999), HB-PLAG (Holland and Blundy, 1994) program is used.

Metamorphic temperature about two places calculates by using an amphibole - plagioclase - quartz geological thermometer (Holland and Blundy, 1994). Because paragenesis metamorphic facies which is used for geobarometer to calculate metamorphic pressure do not discover, geobarometer is calculated by using crossite contents of Ca-hornblende suggested by Brown (1977).

7-1. Geothermobarometery

To assume metamorphic temperature and press in the study, an amphibole - plagioclase - geological thermometer is used. Geological thermometers is made by Holland and Blundy (1994).

In the amphiboles sample mm-9 a, b and mm-10 of Maldo and

mm-27a of Myeongdo, 290~420℃and 570~650℃ (Fig. 35) of temperature conditions are respectively calculated by using the amphibole - plagioclase - geological thermometer. In this study area, metabasites belongs to quartz + albite + amphiboles + epidotes + muscovites + chlorites + pyrite. Also, because there are cross-bedding and graded bedding on the outcrop, it assumes that it is suffered from low metamorphism. So, temperature range (570~650℃) is excepted.

Because paragenesis metamorphic facies which is used for geobarometer to calculate metamorphic pressure do not discover, geobarometer is calculated by using crossite contents of Ca-hornblende suggested by Brown (1976). The result shows ca. 2 kbar (Fig. 36).

Overall, metabasites in this study area is formed at environment of 350℃, ca. 2 kbar (Fig. 37) and assumes buried until 10~15 km.

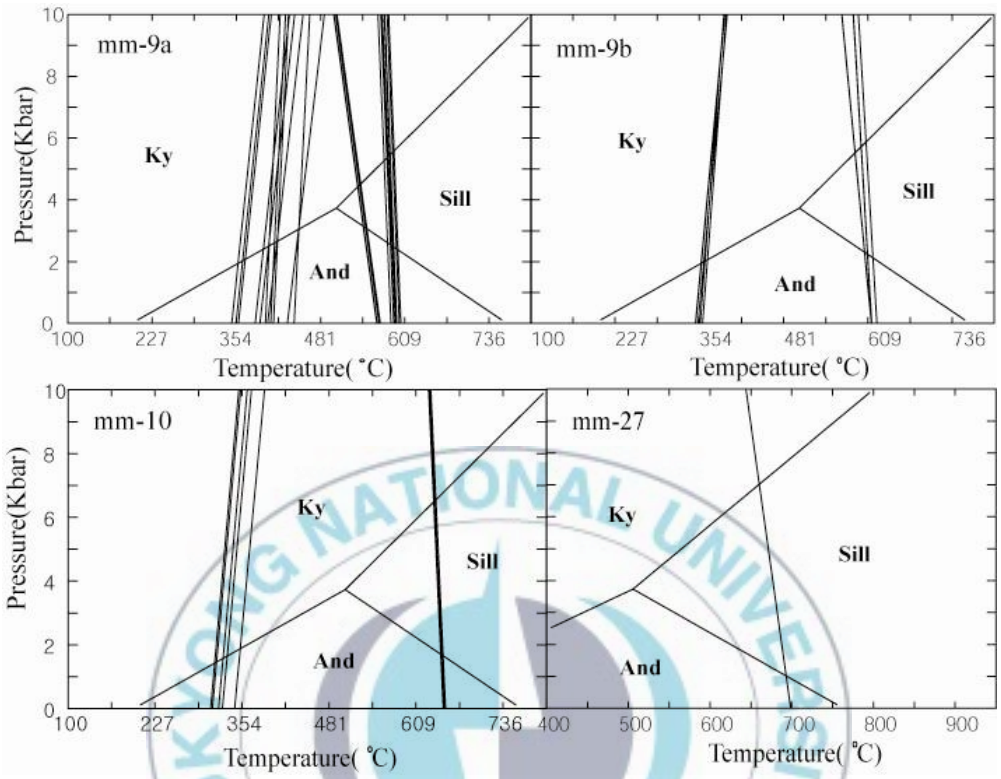

Fig. 35. Results of metamorphic temperature estimates for the metaasites using Hb-Pl geothermometer (Holland and Blundy, 1994).

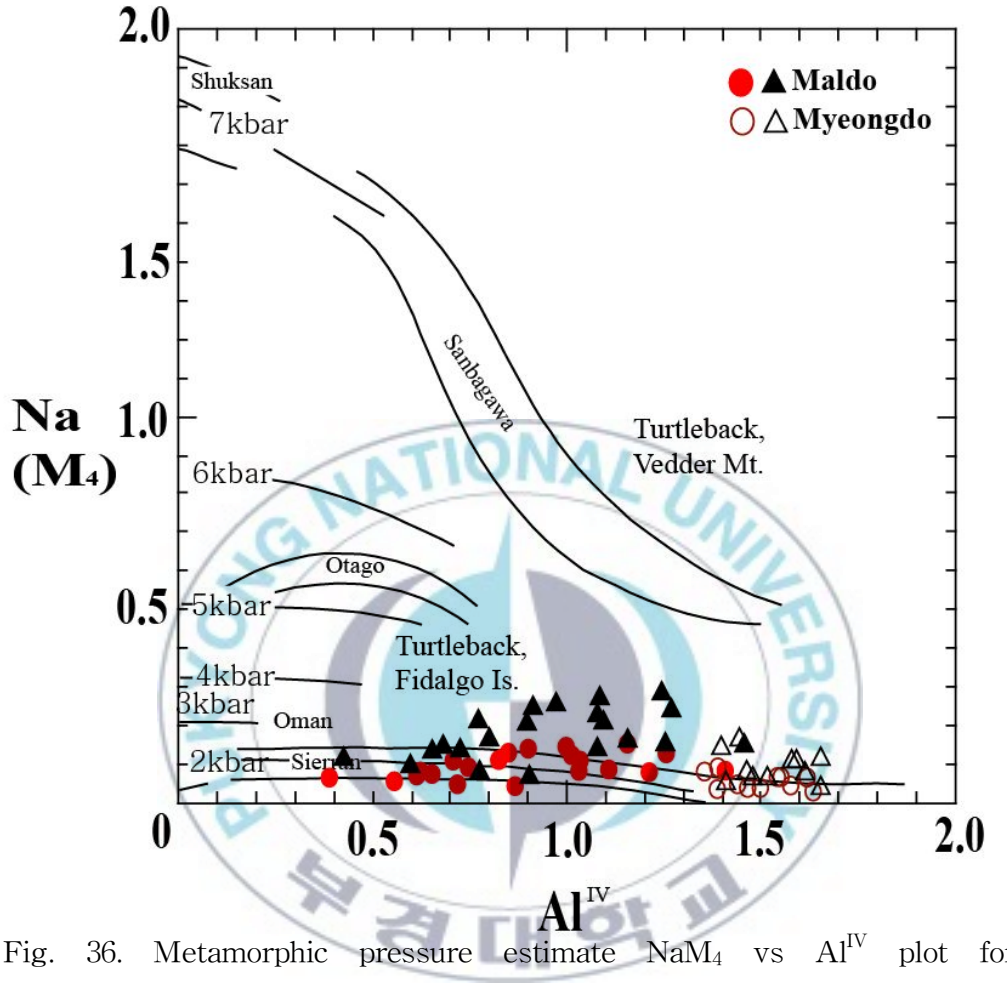

Fig. 36. Metamorphic pressure estimate NaM_4 vs Al^{IV} plot for amphiboles from the metabasites.

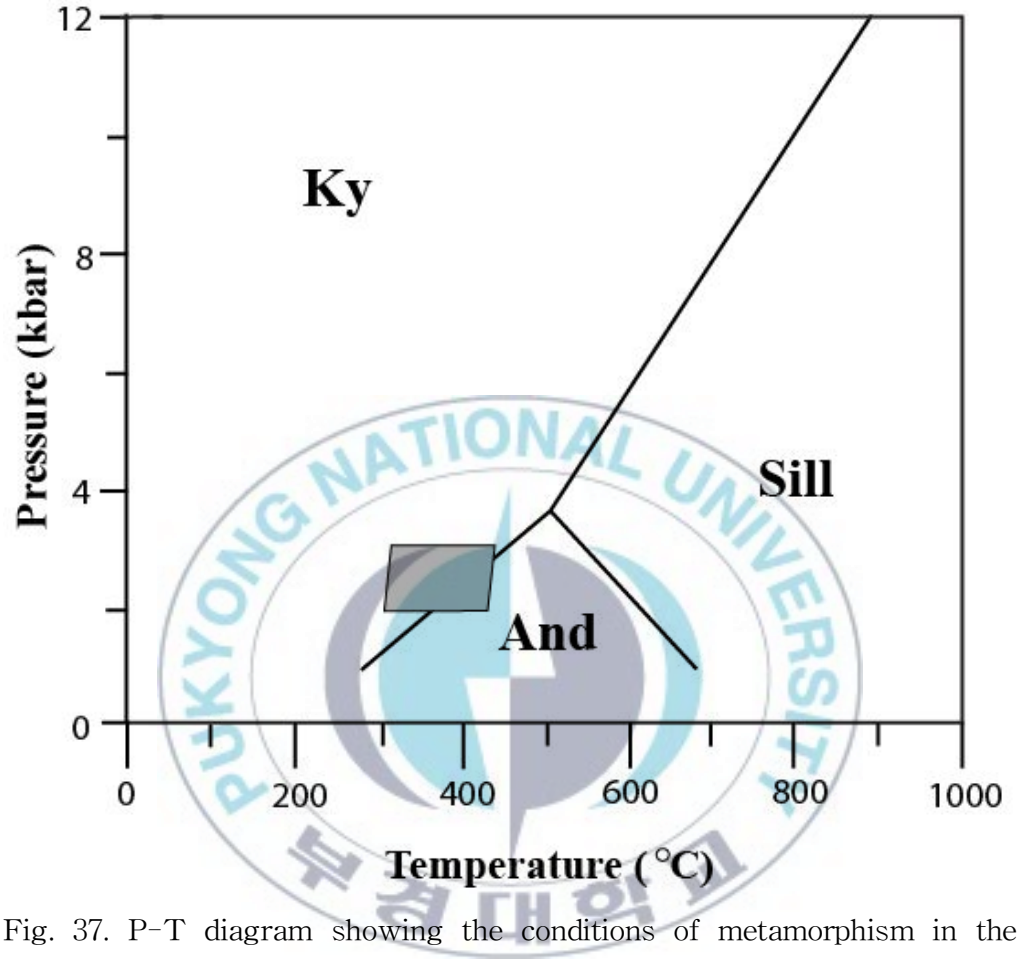

Fig. 37. P-T diagram showing the conditions of metamorphism in the study area based on the estimates using Hb-Pl geothermometer (Holland and Blundy, 1994) and Ca-Amphibole geobarometer (Brown, 1977).

8. Conclusions

Petrological and geochemical studies combined with EPMA analyses of metamorphic minerals were carried out on the low grade metamorphic rocks from the northern part of the Gogunsan Islands on the west of Gunsan city, Jeollabuk-do.

1. Geology of the northern part of the Gogunsan Islands mostly consists of psammitic metasedimentary rocks associated with intercalated metabasite layers and small amount of meta-granites.

2. Although folding and thrust duplex structures were remarkably developed, metasedimentary formations in this area preserve original sedimentary structures including bedding, cross-bedding, graded bedding, ripple marks etc.

3. Major element geochemistry of metasedimentary rocks indicates that the sedimentary basin was supplied with siliciclastic materials derived from continental margin. Geochemical study on meta-granites and metabasites revealed calc-alkaline volcanism and granitic plutonism in a volcanic arc environment.

4. Mineral assemblages of Chl + Ms + Qtz + Pl(Ab) in metasedimentary rocks, Qtz + Kfs + Pl(Ab) + Ms in meta-granites, and Amph(Act to Tschermakite) + Pl(Ab) in metabasites revealed that

metamorphic rocks in this area suffered greenschist facies metamorphism. Hb-Pl thermometer (Holland and Blundy, 1994) and Ca-Amphibole barometer (Brown, 1977) for metabasites suggest that P-T conditions reached about 2 kbar, 350℃.

5. Metasedimentary formations in the study area are considered to be Neo-Proterozoic in age based on their petrographic and metamorphic characteristics.

References

Anderson, J.L., and Smith, D.R., 1995, The effects of temperature and oxygen fugacity on the Al-in-hornblende barometer: Am. Min., 80, 549-559.

An. G.S. and Oh C,H., 2000, Metamorphic Petrology.

Blundy, J.D., and Holland, T.J.B., 1990, Calcic amphibole equilibria and a new amphibole-plagioclase geothermometer. Contributions to Mineralogy and Petrology, 104, 208-224.

Brown, E. H., 1977, The Crossite Content of Ca-Amphibole as a Guide to Pressure of Metamorphism, Journal of Petrology, Volume 18, Number 1, 53-72.

Cabins, B. and Lecolle, M., 1989, Le daigramme La/10-Y/15-Nb/8: un outil pour la discrimination des series volcaniques et la mise en evidence des processus de melange et/ou de contamination crustale. C.R. Acad. Sci.

Cho, M.S., Kim., HC., 2002, Metamorphic Evolution of the Ogcheon Metamorphic Belt: Review of Recent Studies and Remaining Problems, Korea. Jour. Petrol. Soc. Kor. Vol. 11, No .3-4, 121-137.

Cluzel, D., Jolivet, L. and Cadet, J.P., 1991, Early middle Paleozoic intraplate orogeny in Okcheon belt(S. Korea): a new insight on the Paleozoic buildup of east Asiz, Tectonics, 10, 1130-1151.

Cooper, A. F. and Lovering, J. F., 1970, Greenschist amphiboles from Haast river, New Zealand, Contributions to Mineralogy

and Petrology, Volume 27, Number 1.

Davis G.H. and Reynolds, S.J 1996, Structural geology of rocks and regions, John Wiley & Sons Inc., New York, p. 776.

Egawa, K. and Lee, Y.I., 2006, Stratigraphy of the Nampo Group in Ocheon and Odesan area: significance of conglomerates of the Jogyeri Formation for unconformity. Journal of the Geological Society of Korea. Vol. 42, No. 4, 635-643.

Holland, T. and Blundy, J., 1994, Non-ideal interactions in calcic amphiboles and their bearing on amphibole-plagioclase thermometry, Contrib. Mineral Petro. 116, 433-447.

Hong. S.S., 2001, Implication for the emplacement depth of the granites in the Yeongnam Massif, using the aluminum - in - hornblende barometry, Korea. Jour. Petrol. Soc. Kor. Vol. 10, No. 1, 36-55.

Irvine, T.N. and Baragar, W.R.A., 1971. A guide to the chemical classification of the common volcanic rocks. Canadian Journal of Earth Sciences, 8, 523-548.

Jane M. Hammarstrom, E-AN Zen, 1986, Aluminum in hornblende: An empirical igneous geobarometer American Mineralogist, Volume 7 1, 1297-1313

Jang, T.W., Lee, J.Y., Yun, S., 1988, Geological map (1:50,000), Miwon map and description, p.23.

Jeong, G.S. and Kim, J.L., 2000, Sedimentary petrology, 27-243.

Jin. M.S., Choi, H.I., Shin, H.J. and Shin, S.C., 2004, Geological outcrop of Korea, 150, KIGAM.

Kang, J.H., Hara, I., Hayasaka, Y., Sakurai, Y., Shiota, T. and Umemura, H., 1993, Time-relationship between deformation and metamorphism of the Okcheon district, South Korea. Mem. Geol. Soc. Japan, 42, 63-90.

Kang. J.H., 2001, Geological structure of the Ogcheon metamorphic zone in the Busan area, Korea: a new geodynamic model to the Herat - shaped Busan gneiss complex. Petrol. Soc. Kor. Vol. 10, No. 2, 106-120.

Kang. J.H. and Lee C.G, 2002, Geological Structure of Okcheon Metamorphic Zone in the Miwon-Boeun area, Korea. Jour. Petrol. Soc. Kor. Vol. 11, No. 3-4, 234-249.

Kee. W.S.. and Hwang. J.H., 2007, report of geology and mineral cultural heritage, Cultural Heritage Administration of Korea, 31-52.

Koh, H.J. and Kim, J.H., 1995, Deformation sequence and characteristics of the Okcheon Supergroup in the Goesan area, Central Okcheon belt, Korea. Jour. Geol. Soc. Korea, 31, 271-298.

Kohn, M. J. and Spear, F. S., 1999, Probing the depths of Oliverian magmas: Implications for Paleozoic tectonics in the northeastern United States. Geology, 27, 803-806.

Koh. I.S and Shin. Y.S, 1995, Chemical Composition of the Cretaceous Sandstones in Goryeong Area, Southeast Korea. Jour. Korean Earth Science Society, Vol. 16, No. 5, 408-419.

KIGAM, 1995, Geological map of Korea.

Kim. Y.B., Hwang. J.H., Lim. S.B., Kim. D.U., Lee, B.Y., Yu, J.H., Seo, J.L., Kim, Y.Y., Kim, B.C., Kee, W.S., Ko, H,J., Song, K,Y., Jo, D.L.,

Lee, S.L., Lee, S.L., Lee S.L., Kim, Y.H., Shin, J.S., Kim. C.S., 2003, Geolocal survey report of radioactive waste disposal proposed site, KIGAM, p. 273.

Kim. J.Y., 1993, Sedimentary Environment and Stratigraphy of Sedimentary Rocks distributed in Daeheuksan Island, Jour. Korean Earth Science Society, Vol. 14, No. 1, 25-31.

Kim, Y.B., Lim, S.B., Choi, H.I., Lee, C.B., Kim, B.C., Jeon H.Y., Park, S.H., Cho, D.L., Park, H.S., Choi, S.J., Kim, J.C., Ko, H.J., 2000, Stratigraphy of age-unknown strata-southeastern part of Haenam area-, KIGAM, p.126.

Kretz, R., 1993, Symbols for rock-forming minerals, American Mineralogist., 68, 227-279.

Lim, S.B., Choi, H.I., Ko, H.J., 2003, Late mesozoic-Cenozoic tectonic evolution of Korea. 3, KIMGAM.

Leake, B.E., 1964, The chemical distinction between ortho- and para-amphiboles: Jornal of Petrology, 5, 238-254.

Max W. Schmidt Amphibole composition in tonalite as a function of pessure: an experimental calibration of the Al-in-hornblende barometer, Contributions to Mineralogy and Petrology.

Powell, R. and Holland, TJB., 1998, An internally consistent thermodynamic dataset with uncertainties and correlations: 3. Application methods, worked examples and a computer program. J. metamorphic Geol., 6, 173-204.

Powell, R. and Holland, TJB., 1993, The applicability of least squares in the extraction of thermodynamic data from

experimentally bracketed mineral equilibria. American Mineralogist, 78, 107-112.

Robineson, P., Spear, F.S., Schumacher, J.C., Laird, J., Klein, C., Evans, B.W. and Doolan, B.L., 1982, Phase relation of metamorphic amphiboles : Natural occurrence and theory. Reviews in Mineralogy and Geochemistry, Vol. 9B;1, 9-22.

Roser B.P. and . Korsch, R.J, 1986, Determination of the tectonic setting of sandstone - mudstone suites using SiO_2 content and K_2O/Na_2O ratio, Journal of Geology 94 (5), 635 - 650.

Schmidt, M.W., 1992, Amphibole composition in tonalites as a function of pressure : an experimental aslibration of the Al-in-hornblende barometer. Contrib. Mineral. Petrol., 110, 304-310.

Spear, F.S., 1981, An experimental study of hornblende stability and compositional variability in amphibolite. Am. Jour. Sci., 281, 697-734.

Sun S.S. and McDonough, W.F., 1989. Chemical and isotopic systematics of oceanic basalts: implications for mantle composition and processes. in Magmatism in the ocean basins. Geological Society, Special Publication, 42, 313-345.

Song Y.S., Choi J.Y. and Park K.H. The Tectono -metamorphic Evolution of Metasedimentary Rocks of the Nampo Group Outcropped in the Area of the Daecheon Beach and Maryangri, Seocheon-gun, Chungcheongnam-do, Korea. Jour. Petrol. Soc. Kor. Vol. 17, No. 1, 1-15.

Veblen, D., and Ribble, P. (eds.), Amphiboles : Petrology and Experimental Phase relations, Review in Mineralogy Society of America, 1-229.

Wood D.A., 1980. The application of a Th-Hf-Ta diagram to problems of tectonomagmatic classification and to establishing the natute of crustal contamination of basaltic lavas of the British Tertiary volcanic province. Earth and Planetary Science Letters, 50, 11-30.

Abstract

Petrological and geochemical studies combined with EPMA analyses of metamorphic minerals were carried out on the low grade metamorphic rocks from the northern part of the Gogunsan Islands on the west of Gunsan city, Jeollabuk-do. Geology of the northern part of the Gogunsan Islands from Maldo through Myeongdo and Banchukdo to Hoenggyeongdo mostly consists of psammitic metasedimentary rocks associated with intercalated metabasite layers and small amount of meta-granites.

Metasedimentary formations in this study area well preserve original sedimentary structures including bedding, cross-bedding, graded bedding, ripple marks etc. even though folding and thrust duplex structures were remarkably developed.

Geochemistry of metasedimentary rocks, meta-granites and metabasites revealed that the basin was supplied with siliciclastic materials derived from continental margin and accompanied calc-alkaline volcanism and granitic plutonism in a volcanic arc environment.

Greenschist facies metamorphism is indicated by the mineral assemblages of Chl + Ms + Qtz + Pl(Ab) in metasedimentary rocks, Qtz + Kfs + Pl(Ab) + Ms in meta-granites, and Amph(Act to Tschermakite) + Pl(Ab) in metabasites. Geothermobarometry for metabasites suggest that P-T conditions of metamorphic rocks in this area reached about 2 kbar, 350℃.

On the basis of their petrographic and metamorphic characteristics

metasedimentary formations in the study area are considered to be Neo-Proterozoic in age.

감사의 글

논문이 완성되기까지 많은 가르침과 격려를 주신 많은 분들에게 감사의 인사를 드리고자 합니다.

많이 모자란 저를 제자로 받아주시고 지질학이란 학문에 눈을 뜨게 해주신 송용선 교수님께 진심으로 감사드립니다. 교수님의 학문에 대한 열의와 열정은 저에게 많은 채찍질이 되었습니다. 감사합니다. 그리고 항상 저에게 격려를 아끼지 않으셨던 박계헌 교수님께도 감사드립니다. 교수님 덕분에 공부에 대한 자신감이 많이 생겼던 것 같습니다. 또한 바쁘신 와중에도 저의 논문을 심사해주신 김영석 교수님, 지질학에 대해 많은 가르침을 주신 정상용 교수님, 박맹언 교수님, 백인성 교수님, 최정찬 교수님, 이민희 교수님께도 감사의 말씀 전합니다.

대학원 생활에 많은 도움을 주신 연구실의 남훈선배, 호선이 언니. 언제나 많은 충고와 격려로 대학원 생활과 연구실 생활에 많은 도움을 주신 두 분께 정말 감사드립니다. 그리고 자주 찾아뵙진 못했지만 못난 후배를 위해 분석도 도와주시고 가르침도 많이 주신 호정선배님께도 감사의 인사를 전합니다. 지금은 대전에서 열심히 꿈을 펼치고 있을 정윤이 언니와 동혜 언니! 언니들 덕분에 연구실과 대학원 생활에 쉽게 적응도 하고 힘든 일이 있을 때도 많은 도움이 되었습니다. 언니들 절대 잊지 못할 것 같습니다.

타 학교에서 건너와 힘들었을 지완선배. 선배 논문 쓸 때 많이 괴롭혔는데 미안했고, 버릇없는 후배 때문에 선배 많이 힘드셨을 것 같습니다. 그래도 지난 날 연구실의 기나긴 밤을 선배와 함께 보내 즐거웠습니다. 연구실 친구 재현이도 내 논문 도와주느라 많이 힘들었을 거라 생각하는데 정말 고맙고 연구실을 위해 계속 애써주길 바래.

논문 쓰느라 수고한 상건선배, 태영선배, 성수선배, 민준선배, 종성선배,

숙주 모두 수고했어요. 그리고 병우선배, 태형선배, 필근선배, 광민선배, 문호선배, 성일선배, 태호선배, 명진이 언니, 지혜언니, 세영이, 지금은 학교에 없지만 열심히 일하고 있을 주언선배. 모두들 존재만으로도 많은 도움과 위안이 되었습니다.

나의 자랑스러운 친구들. 시영이, 지은이, 경하, 지영이, 희경이, 선영이, 익현이. 모두들 나를 위해 걱정해주고 격려를 아끼지 않은 나의 친구들에게 감사의 인사를 전합니다.

마지막으로 사랑하는 우리 가족에게도 감사의 말을 전합니다. 자랑스러운 딸, 동생이 되겠습니다.